catalysts

MDPI

Review

Carbon-Based Catalysts in Ozonation of Aqueous Organic Pollutants

Petr Leinweber, Jonáš Malý and Tomáš Weidlich *

Chemical Technology Group, Institute of Environmental and Chemical Engineering, Faculty of Chemical Technology, University of Pardubice, Studentská 573, 532 10 Pardubice, Czech Republic; petr.leinweber@student.upce.cz (P.L.); jonas.maly@student.upce.cz (J.M.)
* Correspondence: tomas.weidlich@upce.cz; Tel.: +420-46-603-8049

Abstract

This review summarizes recent applications of carbon-based materials as catalysts in the ozonation of wastewater contaminated with persistent organic pollutants. Methods available for production of commonly used inexpensive carbonaceous materials such as biochar and hydrochar are presented. Differences between production methods of active carbon and biochar or hydrochar are discussed. Interestingly, biochar, in a role of rather simple and cheap charcoal, is catalytically active and increases the rate of oxidative degradation of nonbiodegradable aqueous contaminants such as drugs or textile dyestuffs. This review documents that even the addition of biochar to the ozonized wastewater increases the rate of removal of persistent organic pollutants. Cheap bio-based carbonaceous materials such as biochar work as adsorbent of dissolved pollutants and catalysts for ozone-based degradation of organic compounds via the formation of reactive oxygen species (ROS). Low-molecular-weight degradation products produced by ozonation of pharmaceuticals and textile dyes are presented. The combination of air-based ozone generation, together with application of biochar, represents a sustainable AOP-based wastewater treatment method.

Keywords: ozone; char; active carbon; hydroxyl radical; oxidation; dye; pharmaceutical; wastewater

1. Introduction

Increasing contamination of aqueous resources is a global problem that needs effective sustainable treatment methods to protect limited water sources and remediate contaminated water. Water contamination by persistent organic pollutants—including drugs, common ingredients of cosmetics such as UV filters, dyes, and others—is a growing environmental concern due to their low degradability in common ecosystems and toxic effects on aquatic biota and human health, even at negligible concentrations [1].

Due to these reasons, biological techniques supplemented by different non-destructive physical methods such as adsorption, membrane filtration, as well as destructive chemical reduction or oxidation processes, were studied for effective removal of persistent aquatic pollutants [2].

Most of the above-mentioned methods have considerable limitations. Biological methods are cost-effective and low-energy-demanding; however, their effectiveness is quite limited. Physical methods suffer from low selectivity and production of high quantity of by-products such as concentrates of contaminants. Mentioned chemical methods are often expensive, sensitive to operating conditions and need the secondary treatment.

Academic Editor: Jian Qi

Received: 15 December 2025
Revised: 26 December 2025
Accepted: 27 December 2025
Published: 1 January 2026

Advanced oxidation processes (AOPs) are promising treatment techniques based on action of highly reactive oxidation reagents, such as radicals (most commonly hydroxyl or sulfate radicals) and singlet oxygen ($^1O_2$). These radicals are generated through different mechanisms including photocatalysis, persulfate or Fenton reactions, non-thermal plasma, ozone-based techniques, and their combinations [3].

AOPs achieve oxidative degradation (mineralization) of organic pollutants into harmless products, eliminating the need for subsequent treatment. Cost-effective production of mentioned highly reactive oxidation reagents (hydroxyl radicals or singlet oxygen) is crucial in AOPs [4].

One of the common oxidation processes is based on the action of reactive allotrope of oxygen—triatomic oxygen molecule called ozone. Ozone is the unstable form of oxygen (it is explosive and toxic) produced in ozonators using ambient air or pure oxygen. The two main principles of ozone generation are UV light and corona discharge. Ozone generation by corona discharge is the most common method nowadays and has the greatest advantages. The advantages of the corona discharge method are greater sustainability of the unit, higher ozone production, and higher cost affectivity. UV light can be feasible where production of small amounts of ozone is desired (e.g., laboratories) [5].

The oxidation potential of 2.07 volts proves that ozone is a strong oxidant. In fact, ozone is one of the strongest oxidants available for water treatment. Ozone is rather unstable in an aqueous solution; its half-life in water is about 20 min [6].

An advantage of ozone over other oxidizing agents is that no reduction products remain in the treated medium that would pollute the treated water. During ozonization, the ozone may not be completely consumed, and in that case, the product from the reduction of excess ozone is oxygen, which is freely removed from any product.

Due to the above-mentioned reasons, over the past 50 years, the use of ozonolysis for the degradation of diverse organic substances entering water systems has been investigated—whether these substances originate from dyeing processes, the textile industry, or the washing and processing of textiles [7]; from hospitals, medicine, and the pharmaceutical industry [8–30] (including research on the degradation of genetic material present in wastewaters [31]); or from pollution arising from everyday human activities [32].

An ozone oxidation process is always based on the effect of direct and indirect reaction mechanisms (see Sections 3 and 4).

The direct ozonation is a fairly selective reaction in case of organic substrates. Ozone reacts quickly with organic matter that contains double bonds via formation of ozonides, with activated aromatic compounds such as phenol via electrophilic ozonation and with amines.

The indirect reaction mechanisms are based on OH-radical formation. Contrary to those of ozone, OH-radical reactions are nonselective. Indirect reactions in an ozone oxidation process can be very complex. In general, indirect oxidation can be practically applied to each of oxidizable organic pollutants. Generally, nonbiodegradable organic substances are decomposed to easier biodegradable oxidation products or even completely mineralized in contaminated wastewater.

However, the concentration of OH-radicals produced in aqueous ozone solutions is very low without application of appropriate catalysis. Increased formation of OH-radicals has been observed by action of different transition metal salts.

A wide range of catalysts has also been studied, including metal oxides [9,10,33–44] partially oxidized metallic materials [45], nanomaterials such as nZVI (nano zero-valent iron) [46,47], and other nanomaterials [9,10,21].

On the other hand, most transition metals are potential aquatic pollutants. It means that application of catalysts based on transition metals could cause secondary contamination of treated wastewater [48].

In addition, the efficiency of ozonation is limited by poor ozone gas/liquid mass transfer and low ozone utilization efficiency (typically 30–64% in bubble columns) [5].

Due to the above-mentioned reasons, a suitable additive enabling enhancement of ozone utilization such as an adsorbent and/or catalyst should be very attractive for ozone-based AOPs.

Interestingly, even carbonaceous materials such as active carbon or biochar were recognized as active catalysts for conversion of ozone into OH-radicals and acceleration of oxidative degradation [42–44,49–55].

Carbonaceous materials act as adsorbents of aqueous pollutants and have emerged as catalysts for the formation of hydroxyl radicals by co-action of hydrogen peroxide or ozone [56].

2. Production of Carbonaceous Materials Available as Carbon-Based Catalysts

Waste biomass, such as crop residues, sludge produced in wastewater treatment plants, and solid part of digestate from biogas plants [57], is increasingly used as carbon sources for the production of carbonaceous materials like biochar, hydrochar, charcoal, or active carbon.

The production of biochar relies on a process called carbonization, in which organic matter is exposed to high temperatures (200–900 °C) in the absence of oxygen and converted into carbon-rich solids [58,59]. During this procedure, even other volatile products are also formed, such as bio-oil and syn-gas [58]. The ratio and properties of the resulting products are primarily determined by the feedstock and the specific carbonization conditions, which are discussed later [59–61].

2.1. Difference Between Biochar and Activated Carbon Synthesis

The distinction between biochar and activated carbon is not strictly defined, as their research domains frequently overlap. While both often originate from biomass carbonization, they differ in their specific processing conditions and intended utilizations. Biochar is primarily produced for carbon sequestration or soil amendment. It is also distinct from charcoal; although both originate from similar pyrolytic processes, charcoal is intended for use as a solid fuel for stoves, grills, etc. [62]. Conversely, activated carbon is a high-performance material and relatively expensive carbon-based product used primarily as an adsorbent for the removal of contaminants from gaseous and liquid phases [63].

The utilization of these materials is also related to their energy consumption and carbon footprint. A fundamental prerequisite for biochar utilization is that its production minimizes energy input and achieves nearly neutral carbon footprint. In contrast, activated carbon production is driven primarily by performance properties rather than carbon sequestration goals; as a result, it typically exhibits a positive carbon footprint and a significantly higher energy intensity [64,65].

Biochar is derived exclusively from waste biomass, such as wood shavings or agricultural residues [66]. Biochar is produced via a relatively inexpensive single-step pyrolysis process operating within a temperature range of 200–600 °C (or higher within specific methods) [63]. In contrast, the feedstock for activated carbon includes either non-renewable feedstock sources, such as coal or tar pitch, or renewable, well-defined biomass, such as coconut shells [66]. Unlike biochar, the production of activated carbon involves a secondary step known as activation. This process significantly enhances sorption capacity by developing porosity and increasing the specific surface area [63]. Generally, activation processes

are categorized into two distinct approaches: physical activation and chemical activation. In the physical activation process, the char undergoes controlled partial oxidation using agents such as CO_2 or steam at temperatures ranging from 700 °C to 1100 °C [63,67]. Alternatively, air may be employed as well, provided the process is conducted at lower temperatures (350–550 °C) to prevent uncontrolled combustion [68]. This reaction facilitates the development of new micropores and the enlargement of existing pore structures [63,67]. Chemical activation employs specific chemical agents to facilitate porosity development. It is typically conducted at temperatures ranging from 400 °C to 600 °C. The most prevalent activating agents include alkaline compounds (KOH, K_2CO_3), acids (H_3PO_4, H_2SO_4), and transition metal salts and their combination ($ZnCl_2$/$FeCl_3$) using different feedstocks [69]. This activation method can be conducted via a one-step or two-step process. In the single-step approach, the raw feedstock is impregnated with the chemical agent and heat-treated, resulting in simultaneous carbonization and activation. Conversely, the two-step process involves carbonizing the biomass prior to chemical impregnation and activation [70,71].

Attributable to the additional activation stage, activated carbon exhibits a vastly superior surface area, often exceeding that of biochar by orders of magnitude [65,66,72–74]. Anderson et al. reported that steam activation dramatically increased the specific surface area of biochar derived from mill residues, rising from 15.0 m^2/g to 1283.0 m^2/g. Similarly, for forest residues, the surface area expanded from 11.8 m^2/g to 575.9 m^2/g. These values correspond to increases of 85.5-fold and 48.8-fold, respectively [74]. Activated carbon is also characterized by a higher fixed carbon content and lower ash content than biochar [75]. Conversely, biochar retains a higher concentration of oxygen in the form of surface functional groups, such as phenolic and carboxylic acid groups [76].

As was mentioned above, biochar lacks high surface area and chemical stability compared with active carbon. To enhance the performance of biochar in water treatment applications, various modification techniques are sometimes used to increase its catalytic activity and pollutant removal efficiency [56] (see Section 4 for more details).

2.2. Biochar Feedstock

The primary feedstock for biochar production is biomass, defined as organic matter derived from animals, plants, and microorganisms. The most fundamental classification of biochar feedstock distinguishes between woody and non-woody biomass. Woody biomass is typically characterized by low moisture and ash content, coupled with high bulk density and calorific value. Conversely, non-woody biomass generally exhibits the opposite physicochemical properties, including higher moisture levels, greater ash content, and lower density and energy density [77]. Biomass can be also classified into four generations based on its origin. The first generation consists of starch-rich edible crops such as corn, potatoes, rice, and wheat. However, due to global food security concerns, utilizing these crops for non-food applications is generally discouraged. Second-generation biomass, often termed lignocellulosic biomass, is primarily composed of cellulose, hemicellulose, and lignin. Examples include wood, sawdust, straw, grasses, and agricultural residues. Due to its high abundance and cost-effectiveness compared to first-generation crops, it is considered an ideal feedstock for biochar production. Third-generation biomass refers to algae, which is valued for its rapid growth rates and, unlike the second generation, its considerable protein content [73]. However, a significant limitation of this feedstock is its high moisture content and production cost [78]. Finally, a fourth generation is often distinguished; this category encompasses organic wastes such as fruit and vegetable residues, nut shells, and spent coffee grounds [73,79,80].

Moisture content is a critical parameter for biochar feedstock using the above-mentioned pyrolysis method. Biomass holds water in various forms, including free water,

water vapor, and bound water within the pore structure [81] (see Table 1). High moisture content is unfavorable, as it significantly increases the energy input required to reach desired temperatures [82]. Consequently, the moisture content in pyrolysis feedstock should not exceed 30% [61].

Table 1. Biochar production methods.

Biochar Production Method	Suitable Feedstock Moisture	Process Temperature	Residence Time	Biochar Yield	Lit.
Slow pyrolysis	Low to medium	400–600 °C	hours to tens of hours	30–55%	[78,83]
Intermediate pyrolysis	Low	500–650 °C	<30 min	15–25%	[80,83,84]
Fast pyrolysis	Low	850–1250 °C	0.5–10 s	10–25%	[80]
Flash pyrolysis	Low	900–1200 °C	0.1–1 s	11–22%	[78,80]
Gasification	Low to medium	700–1200 °C	Depending on the reactor type	5–15%	[85,86]
Torrefaction	Low to medium	200–300 °C	10–60 min	65–95%	[61,87]
Hydrothermal carbonization	High	180–260 °C (+pressure)	hours to tens of hours	50–80%	[81,88]

Furthermore, moisture content indirectly influences char formation and aromaticity. High moisture levels consume thermal energy during the drying phase, thereby reducing the effective duration of pyrolysis. Conversely, lower moisture content allows for a longer effective pyrolysis period, promoting carbonization and the development of polyaromatic and graphite-like surface structures [82]. For biomass with high content of water, hydrothermal carbonization (HTC) is the preferred conversion pathway for producing carbon-rich hydrochars, as it eliminates the need for energy-intensive pre-drying [89,90].

2.3. The Effect of Pyrolysis Conditions

Pyrolysis, the predominant method for biochar production, is defined as the thermochemical decomposition of biomass in an inert or oxygen-limited atmosphere [80]. During this process, other valued products besides biochar arise, such as syngas and bio-oil [81]. Pyrolysis is performed in the temperature range of 300–1200 °C, which can be adjusted to optimize the ratio of these products [80,85]. The process of pyrolysis can be divided into distinct stages. The first stage, known as pre-pyrolysis (up to 200 °C), involves the evaporation of moisture and light volatiles. At moderate temperatures (200–300 °C), cellulose and hemicellulose begin to decompose, although the char retains remaining volatile matter and functional groups containing oxygen [58,82,91]. Approximately at 300 °C, hemicellulose and the majority of cellulose have already decomposed. At medium temperatures (300–500 °C), devolatilization and decomposition of biomass proceed rapidly, forming char and permanent gases, such as carbon monoxide (CO), carbon dioxide (CO_2), hydrogen (H_2), and methane (CH_4) [80,87]. Lignin undergoes thermal degradation more slowly than cellulose and requires higher temperatures, with significant conversion occurring in the 300–600 °C range. As temperatures rise, the biomass structure cracks, releasing volatile compounds. Consequently, syngas production increases while biochar yield decreases [61,92]. The bio-oil production peaks at approximately 500 °C, with its yield reducing at higher temperatures [85]. Above this threshold, the surface area and porosity significantly increase due to the breakdown of structure and micropore development [82]. Simultaneously, the content of fixed carbon and aromaticity rise, which results in enhanced stability [66]. Thermal degradation also affects chemical composition. Oxygen-containing functional groups

(carboxyl, hydroxyl, and carbonyl) decompose, reducing cation exchange capacity and increasing hydrophobic character [93]. This transformation is reflected in the elemental molar ratios: both O/C and H/C ratios decrease, indicating higher aromaticity. Biochars with an O/C ratio below 0.2 are considered highly stable (suitable for carbon sequestration), while those between 0.2 and 0.6 are moderately stable, and those above 0.6 are relatively unstable [94].

Based on process conditions, pyrolysis is categorized into four main types: slow, intermediate, fast, and flash pyrolysis. Slow pyrolysis operates at low heating rates and temperatures ranging from 400 °C to 600 °C, with residence time extending from hours to tens of hours [83]. Notably, this process is partially self-sustaining, as the thermal decomposition of biopolymers is an exothermic reaction. Among all pyrolysis methods, slow pyrolysis produces the highest char yield (30–55%). The resulting biochar is characterized by high aromaticity and stability, making it an ideal choice for carbon sequestration [78]. Intermediate pyrolysis is designed to create a balance between solid and liquid products, avoiding high yields of one product at the expense of the other, as is the case with other types of pyrolysis [80]. The operating temperature of intermediate pyrolysis is typically 500–650 °C with a residence time up to 30 min [80,83]. The typical product distribution for this process is approximately 40–60% bio-oil, 20–30% syngas, and 15–25% biochar [84]. The advantage of intermediate pyrolysis is the ability to process a wide range of biomass from various sources [61]. Fast pyrolysis is characterized by rapid heating rates and very short residence times [72]. Fundamentally, the process aims to heat biomass to thermal cracking temperatures while minimizing exposure time in order to suppress char formation [80]. Consequently, fast pyrolysis maximizes the yield of liquid and gaseous fractions, with the specific output dependent on the operating temperature. To target bio-oil production, which is the most common application, the feedstock is subjected to moderate temperatures (450–650 °C) for a residence time of 0.5–10 s [95]. Conversely, when the desired product is syngas, the operating temperatures can exceed 1000 °C. To facilitate rapid heat transfer, this process requires feedstock with low moisture content (<10%) and fine particle size (finely ground) [96]. Flash pyrolysis represents an intensified variant of fast pyrolysis, characterized by extremely high heating rates and residence times shorter than 1 s. Operating temperatures typically range from 900 °C to 1200 °C [92]. While this process maximizes bio-oil production, it results in minimal biochar and syngas yields [80]. However, the quality and stability of the liquid product present a challenge, as undesirable polymerization reactions, often catalyzed by fine char particulates, can lead to increased viscosity [61,80].

2.4. Biochar Produced as a By-Product of Gasification

Gasification is a thermochemical process defined by the thermal conversion of biomass through partial oxidation [97]. The major product of this process is syngas, a mixture consisting primarily of H_2 and CO, with minor constituents including CO_2, CH_4, and higher gaseous hydrocarbons [98]. In addition to syngas, the process generates several byproducts, including char, bio-oil, tars, and ash [97,98]. Gasification generally occurs in four stages: preheating (drying), devolatilization (pyrolysis), oxidation (combustion), and reduction (gasification). During the preheating phase, the feedstock is subjected to temperatures below 150 °C, causing moisture to evaporate as steam [99]. In the pyrolysis phase, temperatures rise to approximately 700 °C, resulting in the thermal degradation of the biopolymer structure and the release of volatile matter and liquid tar [99,100]. Within the oxidation phase occurs partial oxidation of pyrolysis products to CO_2 and H_2O. Since oxidation is an exothermic process, reaction temperatures typically reach up to 1200 °C [86]. During the endothermic reduction phase, combustion gases generated in the oxidation phase react with the remaining char to yield the primary constituents of syngas (CO

and H_2) [101]. Since biochar yields from gasification are typically limited to 5–15%, this method is generally considered inefficient for applications where biochar is the primary target [85,91].

2.5. Torrefaction for Biochar Production

Torrefaction, often referred to as mild pyrolysis, is a low-temperature thermochemical conversion process. It is typically conducted in the temperature range of 200–300 °C in the absence of oxygen [102]. Typical residence times range from 10 to 60 min, although some sources report durations of up to 120 min [61,103]. The torrefaction process is typically divided into five distinct stages: heating, pre-drying, post-drying, torrefaction, and cooling. The initial heating and pre-drying stages are primarily dedicated to moisture removal. The post-drying phase involves the vaporization of residual moisture and initial decomposition of biopolymers [104]. Finally, the torrefaction phase reaches the peak process temperature, resulting in the extensive thermal degradation of the hemicellulose and a partial decomposition of the cellulose and lignin [105]. The mass yield of the solid product typically ranges from 65% to 95%, with the balance comprising gases and liquid volatiles. This solid fraction consists of largely preserved lignin and cellulose, along with non-volatile byproducts of hemicellulose decomposition [87]. While the low processing temperatures of torrefaction limit physical pore formation, they ensure the preservation of oxygenated functional groups that are crucial for specific adsorption pathways [102]. Based on process conditions, different variants of a torrefaction can be distinguished, including wet, steam, or microwave-assisted torrefaction [88].

2.6. Hydrothermal Carbonization

Hydrothermal carbonization (HTC) is a thermochemical conversion technique uniquely suited for high-moisture biomass (algae, sewage sludge, etc.). In this process, feedstock is treated in subcritical water, yielding a solid carbonaceous product known as hydrochar [89]. The process is conducted in an aqueous environment at temperatures ranging from 180 °C to 260 °C and under elevated pressures (2–6 MPa) [88,90]. Under these conditions, the physicochemical properties of water undergo significant changes, leading to elevated concentrations of H_3O^+ and OH^- ions. Consequently, the water acts as an acid-base catalyst for hydrochar formation [89]. The biomass constituents (hemicellulose, cellulose, and lignin) undergo a complex reaction network initiated by hydrolysis into monomers and oligomers. This is followed by dehydration, fragmentation, polymerization, and condensation, ultimately yielding hydrochar [58]. Compared to biochars produced via pyrolysis, hydrochars exhibit inherently lower surface area and porosity, limiting their effectiveness in physical adsorption [90]. However, oxygenated functional groups are mostly preserved, which results in an elevated ion-exchange capacity [58].

3. Role of Carbocatalysis in Ozonation Processes

Carbocatalysis refers to the application of carbonaceous materials as metal-free catalysts to facilitate chemical reactions, particularly in the field of advanced oxidation processes (AOPs) for wastewater treatment [106]. For a long time, transition metals have been employed as an activator for oxidizing agents (peroxymono-sulfate (PMS), peroxydisulfate (PDS), hydrogen peroxide (H_2O_2), or ozone) to generate highly reactive oxygen species (ROS), such as sulfate radical ($SO_4^{\bullet -}$), hydroxyl radical (•OH), and superoxide radical ($O_2^{\bullet -}$). While highly effective, traditional metal-based catalysis relies on various metal elements that often act as a source of secondary pollution [107]. Consequently, research has shifted toward metal-free, environmentally friendly alternatives, specifically carbonaceous materials such as activated carbon and biochar (Scheme 1).

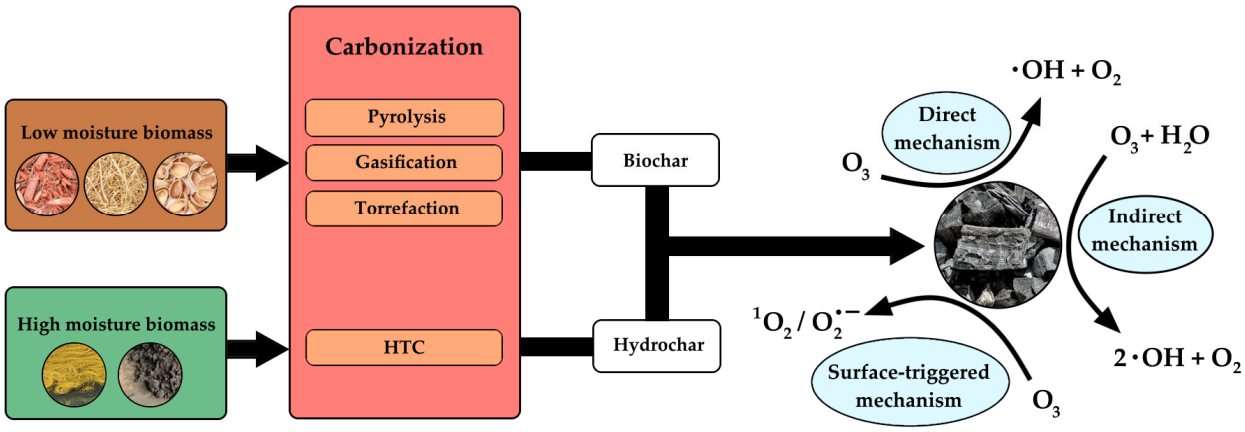

Scheme 1. Preparation of biochar and its catalytic aplication in ozone-based oxidations.

In the field of carbocatalysis, two primary reaction mechanisms are distinguished: radical and non-radical pathways. The radical pathway involves the catalytic generation of reactive radical species (e.g., hydroxyl or sulfate radicals) at the catalyst's active sites. These radicals oxidize pollutants significantly more effectively than the precursor oxidant [106,108,109]. During the carbonization process, four intrinsic structural features develop that function as active sites: persistent free radicals (PFRs), oxygen-containing functional groups (OCFGs), graphitic structures, and defective structures [110]. PFRs are typically generated during pyrolysis at approximately 400 °C, involving electron transfer mechanisms from precursors such as phenols and quinones [108,111]. However, PFRs are metastable and gradually decay upon exposure to atmospheric oxygen, with lifetimes ranging from hours to months [54]. Functioning as electron donors, these structures activate oxidants such as hydrogen peroxide (H_2O_2) or persulfate (PS), resulting in the formation of reactive oxygen species (ROS) [50]. PFRs are classified into three groups: oxygen-centered, carbon-centered, and oxygenated-carbon-centered radicals [54]. Oxygen-containing functional groups (OCFGs) are also frequently generated during mild temperature pyrolysis [110]. These structures, including carboxyl, phenolic, lactone, ketonic, and hydroxyl groups, act as active sites for electron transfer, thereby catalyzing the generation of reactive species such as radicals or singlet oxygen from oxidants [106,107,110,112,113]. Consequently, OCFGs facilitate both radical and non-radical pathways, depending on the specific interaction between the functional group and the oxidant [110,114]. In parallel, structural defects, such as edge defects (zigzag or armchair configurations) and topological defects (non-hexagonal rings), represent disruptions in electron conjugation and possess unpaired electrons [106,111]. Therefore, these high-energy sites are prone to triggering radical formation upon contact with an oxidant [106,113]. Conversely, ordered graphitic structures enhance the material's electron conductivity, functioning as a transfer medium. This conductivity facilitates Direct Electron Transfer (DET) between the contaminant and the oxidant, a mechanism essential for non-radical degradation pathways [106,114,115].

The abundance of specific active sites depends primarily on the pyrolysis temperature. Biochar produced at mild temperatures (<400 °C) is characterized by a high concentration of OCFGs and oxygen-centered PFRs [112,116,117]. At this stage, the carbon matrix is predominantly amorphous and disordered [66]. As temperatures rise to a moderate range (400–600 °C), OCFGs degrade rapidly, leaving behind areas with structural defects [72,110,116]. Besides that, oxygen-centered PFRs gradually transform into carbon-centered PFRs, while the total radical concentration begins to decline [112]. During this phase, amorphous carbon starts converting into poly-aromatic domains, making defects more abundant [66]. Biochar produced at high temperatures (>600 °C) exhibits a high

degree of graphitization. At this stage, the material contains negligible OCFGs and a significantly reduced population of carbon-centered PFRs, with structure being mostly transformed from amorphous into graphitic [72,93,115].

4. Mechanisms of Direct Ozonation

The reaction of ozone with an unsaturated, generally non-aromatic organic framework enables, through the oxidative action of ozone, the formation of a molozonide (Scheme 2) and subsequently—after cleavage of the original unsaturated chain—a wide spectrum of aldehydes, ketones, and in some cases also carboxylic acids. This type of reaction is typically very non-selective, and the product distribution strongly depends on the nature of the multiple bonds present in the structure, their substitution pattern, the apparatus used, the amount of ozone that can be generated and introduced into the solution, as well as parameters such as temperature and even pH [118]. On the other hand, non-selectivity of ozone-based oxidation and high reactivity of ozone are broadly utilized for non-biodegradable aqueous organic contaminants. The above-mentioned oxidation products (aldehydes, ketones, and carboxylic acids) are often more easily biodegradable compared with starting organic compounds.

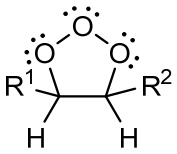

Scheme 2. Structure of molozonide.

Harries investigated the action of ozone on aqueous solutions of various unsaturated organic compounds, particularly substituted alkenes, for example oxidation of isoeugenol—propene-substituted guaiacol—to vanillin earlier published by Schönbein, Bathold, and Dieckhoff (Scheme 3) [119].

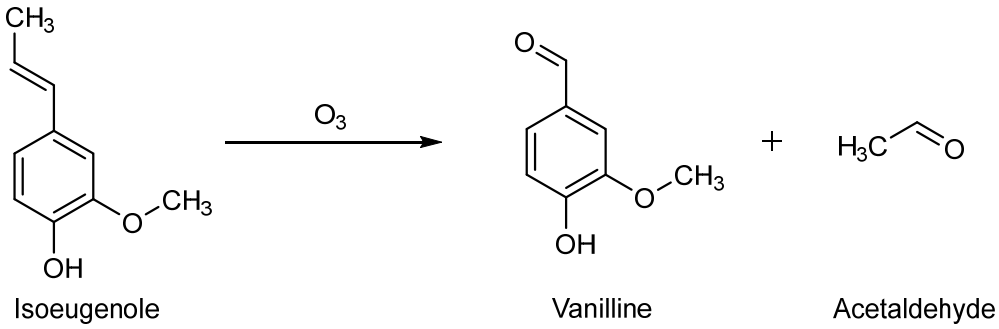

Scheme 3. Ozonolysis of isoeugenol to vanillin [119].

Investigations by Harries represented the first steps toward understanding the mechanism of ozonization. The next breakthrough came with the work of R. Criegee [120], who carried out the first true mechanistic studies of ozonolysis, enabled by the discovery of the structure of ozonides [121] as 1,2,4-trioxolanes—five-membered cyclic organic peroxides formed via ozonolysis of alkenes (Scheme 4).

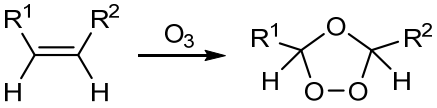

Scheme 4. Formation of ozonides by ozonization of alkenes.

Criegee and Schröder finally characterized an ozonization product that clearly confirmed the formation of a molozonide (1,2,3-trioxolane). Prior to these experiments, five potential primary products of ozonolysis had been considered (Scheme 5) [120]:

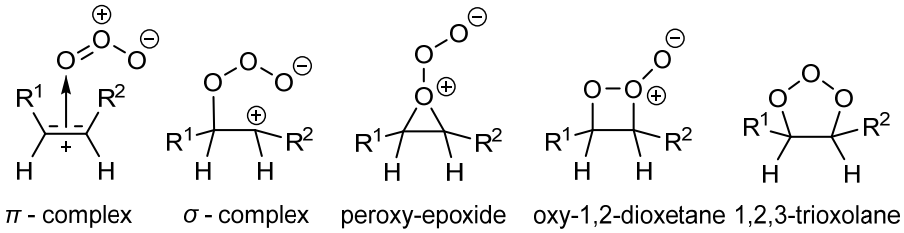

Scheme 5. Possible primary ozonolysis products prior to the discoveries of Criegee and Schröder [120].

Primary ozonides exhibit stability only at very low temperatures, usually far below –78 °C. To rationalize the broad range of decomposition products, Criegee and Werner proposed that the molozonide undergoes an extremely rapid fragmentation in which the C–C and O–O bonds are cleaved, while the stronger C–O bonds remain intact. This rearrangement yields an aldehyde and the zwitterionic Criegee intermediate (Scheme 6) [122]:

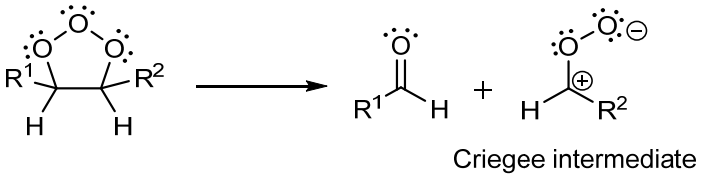

Scheme 6. Formation of the Criegee intermediate [120].

The Criegee intermediate formed is analogous to a nitroso substituent and, like the nitroso group, can engage in resonance stabilization (Scheme 7) [120].

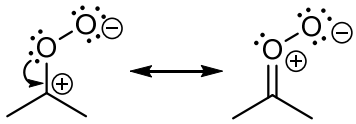

Scheme 7. Zwitterionic ion stabilization through rezonation [120].

These zwitterionic species can undergo stabilization through several pathways. When the parent alkene is tetrasubstituted at the double bond, the steric stabilization enables dimerization of the zwitterions, yielding 1,2,4,5-tetraoxanes [123] (Scheme 8):

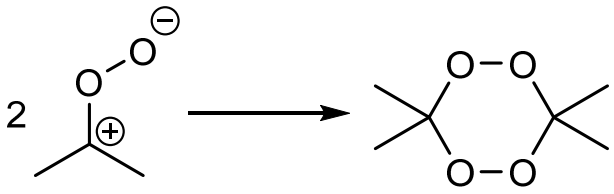

Scheme 8. Dimerization of Crieege intermediates formed by ozonolysis of tetrasubstituted alkenes [123].

The chemistry of Criegee intermediates is remarkably rich and has been thoroughly explored over the past five decades (Scheme 9). Their potential reaction pathways include the following: (a) reduction, (b) cykloaddition, (c) epoxidation, (d) reactions with nucleophiles, (e) oxidation of thioketones to sulfur analogues of the Criegee intermediate

through oxygen-radical transfer, and (f) isomerization of Criegee intermediates to form hydroperoxides and cyclic ozonides [124].

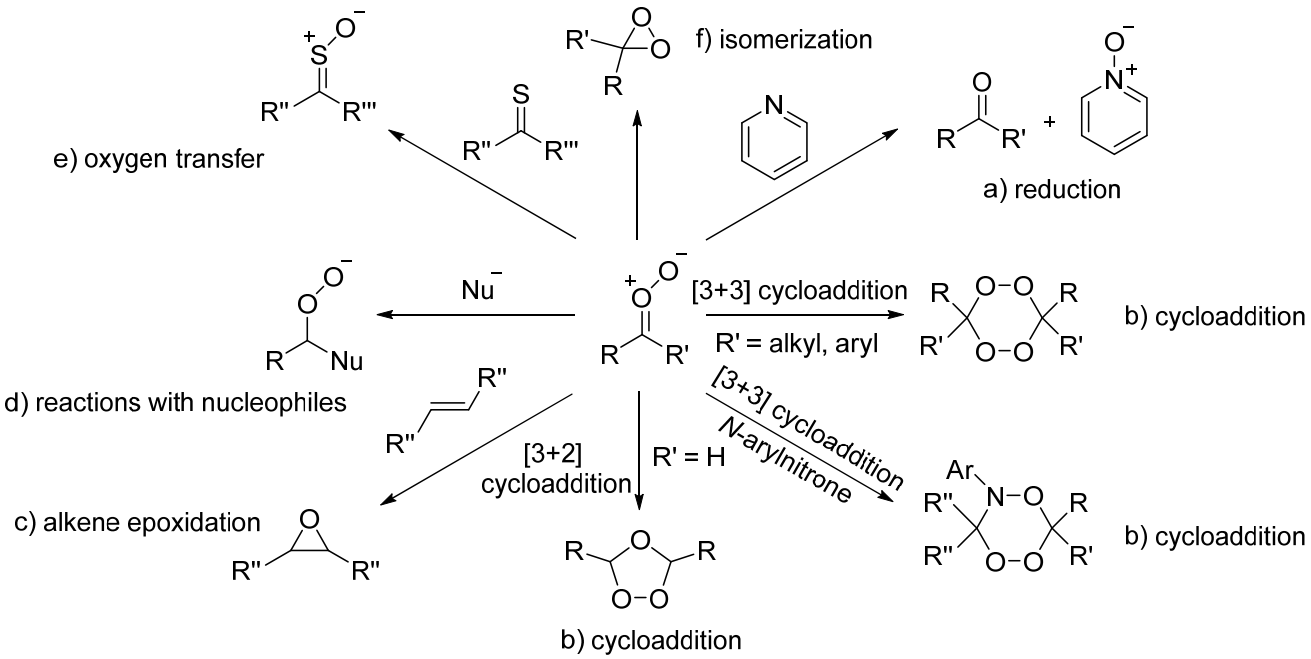

Scheme 9. Selected reaction pathways of Criegee intermediates [124].

5. Role of Catalysis in AOPs Using Ozone

5.1. Ozonation of Pharmaceutical and Hospital Waste Streams

Experimental data indicate that the degradation of pharmaceutical and hospital effluents represents one of the most promising fields for the application of ozonation. Medical and pharmaceutical facilities generate a broad spectrum of contaminants that not only are poorly biodegradable but also can disrupt the biological treatment stages of wastewater plants—antibiotics being the classic example [8–31] (Scheme 10). Ozonation, therefore, emerges as a logical first-line treatment for such wastewater. Importantly, ozonation has also proven capable of removing nanogram-per-liter levels of biologically active compounds from waters not directly linked to pharmaceutical manufacture or hospital discharge [13]. Szabová et al. investigated the ozonation of real wastewater containing a mixture of pharmaceuticals and related residues at concentrations ranging from several hundred ng/L up to 1800 ng/L. Among the monitored pharmaceuticals were diclofenac, telmisartan, sulfapyridine, metoprolol, bisoprolol, sotalol, and tramadol—over twenty compounds in total. Using an ozone input of 50 mgO_3/min, the process achieved 99% removal within ten minutes, with a 97% decrease already observed after the first minute [13] (Table 2).

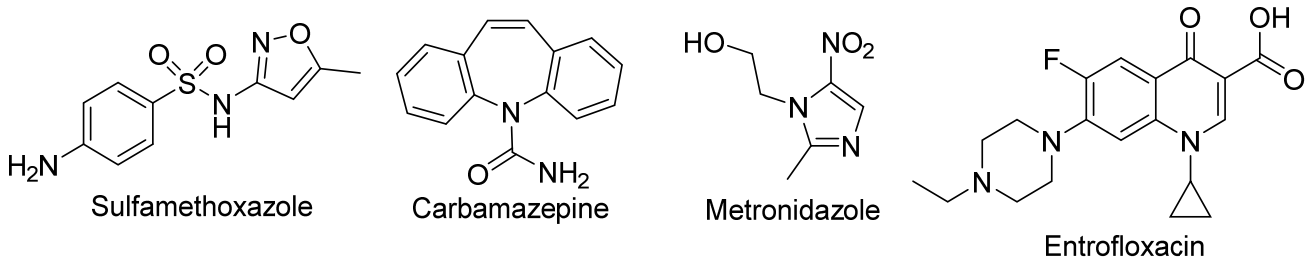

Scheme 10. Structures of several pharmaceuticals that have been studied for their susceptibility to degradation by ozonolysis [9,125,126].

Table 2. Removal of pharmaceuticals from wastewaters via ozonolysis. For detailed data and methodological context, readers are referred to the study by Szabová et al. [13].

	t = 0 min ng/L	t = 1 min ng/L	t = 10 min ng/L	Removal Eff. %
Telmisartan	1800	30	4.6	99.7
Diclofenac	680	<0.4	<0.2	>99.9
Fexofenadine	620	4.8	14	97.7
Irbesartan	400	13	<1.2	>99.7
Tramadol	360	<3.8	<2	>99.4
Cetirizine	260	<3	<1.6	>99.4
Metoprolol	220	<3.2	<1.8	>99.2
Sulfathiazole	160	<3.4	<2.6	>98.4
Azithromycin	150	<13	<12	>92.0

Beyond these relatively low-concentration aqueous pharmaceutical solutions, a substantial number of studies have investigated the degradation of biologically active compounds in water systems where such substances are present at much higher concentrations. This includes both pharmaceuticals themselves and substances used, for example, as disinfectants, such as phenol [127].

The long-term research interest in the removal of these compounds has made it possible to assess the influence of a wide range of operational parameters, including ozone dosage, solution pH, initial contaminant concentration, and the presence of various catalysts (e.g., for sulfamethoxazole or the antiepileptic carbamazepine [125]). Our literature survey shows that catalytic ozonation has been especially well studied for ciprofloxacin and its N-ethyl derivative, as well as for the veterinary antibiotic enrofloxacin. These compounds can serve as benchmark systems for comparing different ozonation strategies, both in controlled model waters [9,126] and in real wastewater environments [63]. The high efficiency of ozone in pharmaceutical removal is further underscored by successful trials conducted on prototype wastewater treatment plant systems [128] (Table 3).

Table 3. Comparison of selected experiments with Ciprofloxacin and [9].

	Conc. [mg/L]	Ozone Dosage [mgO_3/L·min]	pH	Catalyst	Duration of the Zonation Process [min]	Removal by A in UV [%]	Lit.
Ciprofloxacin	80	15 mg/L	7.45	-	10	70	[11]
	80	15 mg/L	7.45	Biochar	10	92.5	[11]
	10	0.4	7	-	15	~25	[12]
	10	0.4	7	MWCNT	15	67	[12]
	10	0.4	7	MnOx MWCNT	15	86	[12]
	10	1.4	9.5	γ-Al_2O_3 (20 nm)	60	93	[9]
	50	1.4	9.5	γ-Al_2O_3 (20 nm)	60	55.1	[9]
	10	1.4	9.5	-	60	88	[9]
	50	1.4	9.5	-	60	~ 53	[9]
	50	C_{O3} = 13.67 mg/L	10.26	Mn-CeO_x γ-Al_2O_3	60	99	[10]

The catalysts explored for these applications span a wide range—from activated and doped alumina materials [9,10] to $Mg(OH)_2$ immobilized on magnetic supports, which greatly enhanced the ozonation efficiency toward metronidazole [21]. Biochar [11], mul-

tiwalled carbon nanotubes (MWCNTs) [12], activated carbon and other carbon-based materials, both undoped and doped, have also been extensively investigated [27–29].

The data in Table 3 indicate that ozonation efficiency depends strongly on the initial contaminant concentration and, in particular, on pH. A similar behavior was observed for a real sludge sample from a wastewater treatment plant in Istanbul, which was resuspended in water and adjusted to pH values between 4 and 11.5. Under acidic and mildly acidic/neutral conditions (pH 4 and 6.5), less than 25% of ciprofloxacin was degraded after 30 min, whereas at pH 11.5 the degradation reached 98% within the same period. This pronounced enhancement is attributed to the increased reactivity of ciprofloxacin toward ozone and hydroxyl radicals at elevated pH [22].

Thanks to modern analytical methods, it is also possible to monitor the composition of the mixture of decomposition products resulting from ozonolysis, as was the case, for example, in the study by Adamek et. al, who identified decomposition products of four antibiotics in this way [14]. Oxidation products of sulfathiazole are depicted in Scheme 11.

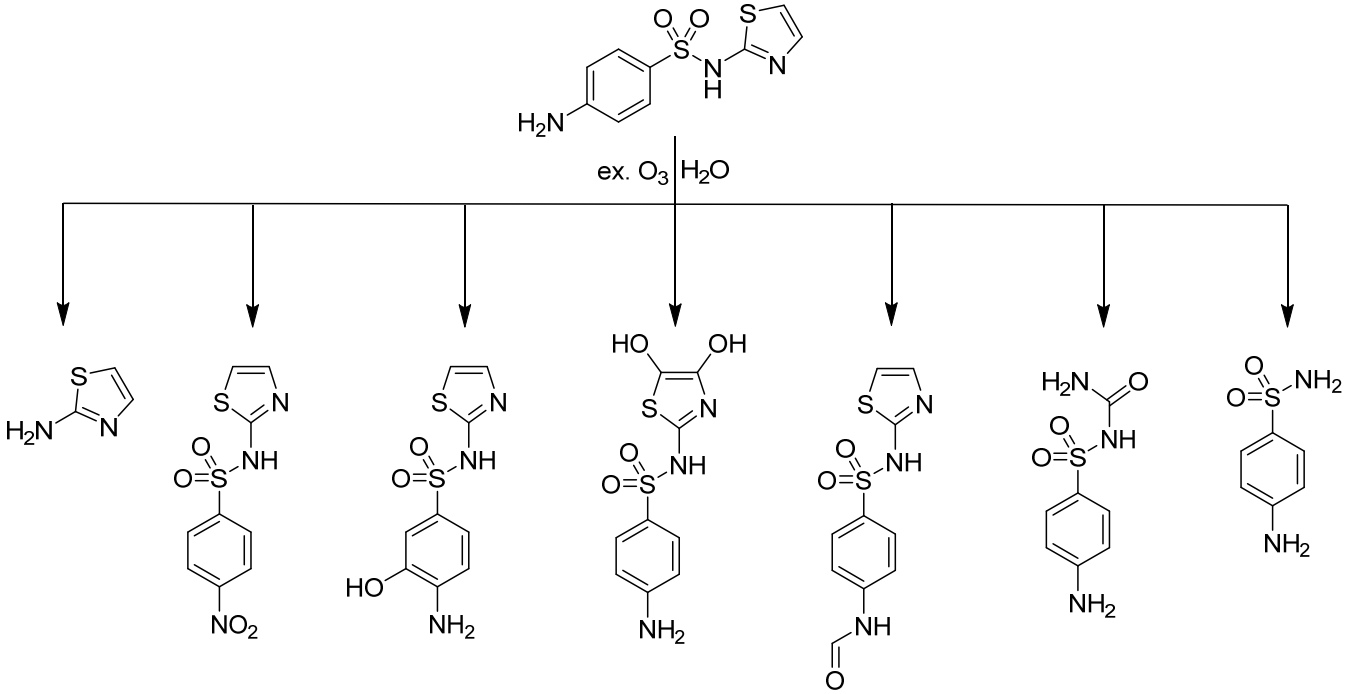

Scheme 11. Examples of products of sulfathiazole ozonolysis [14].

5.2. Ozonation of Dyes-Containing Aqueous Solutions

More than 100,000 tons of dyes are released into aquatic systems each year through dyeing operations [129], and the ozonation of many of these dyes has become a well-established area within advanced oxidation research. Over the past five decades, the degradability of a wide range of dye classes—including acidic, direct, disperse, and reactive dyes—has been examined. Certain dyes, such as Reactive Black 5, Reactive Blue 19, and Acid Blue 113 (Scheme 12), have received particularly extensive attention due to their relatively rapid and straightforward degradation behavior. While this may appear to be a limitation, it is in fact highly advantageous, because we are able to compare different modifications of ozonation. In the last twenty years, research has expanded far beyond simple ozonation to include homogeneous catalytic systems (for example use of TAED—tetraacetylethylenediamine [130]) and numerous heterogeneous catalysts based on carbon materials (activated carbon [40,50,51,131], biochar [53], carbon nanotubes [52], and carbon-metal oxides composites [132]), as well as activated metal oxides, their doped

variants and nanomaterials [36–39]. Additional developments include ozonation assisted by co-oxidants, such as hydrogen peroxide, and photocatalytic processes—primarily TiO_2-based systems [133,134]. These advances now allow for a comprehensive evaluation of how such modifications influence both the rate and efficiency of dye degradation, not only in terms of color removal but also in reductions of Chemical Oygen Demand (COD) and Total Organic Carbon (TOC).

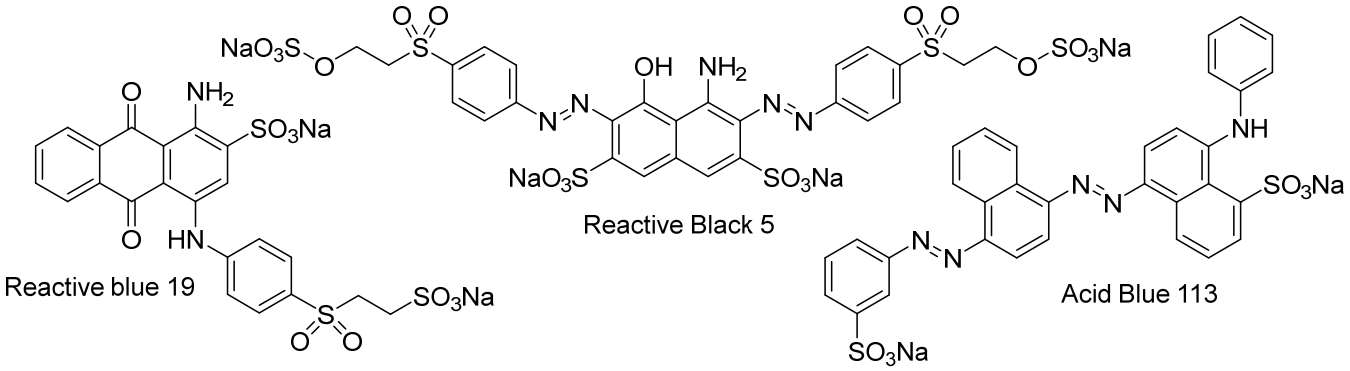

Scheme 12. Selected textile dyes.

5.3. Ozonolysis of Acid Blue 113

This dye is a typical acid azo dye with an absorption maximum at 566 nm [42]. Due to its extensive industrial use and high relevance over the past two decades, the degradation of this dye in wastewater has been the subject of active research employing a broad array of methods. These include biological treatments involving microorganisms, such as *Pseudomonas* [135] and *Bacillus* species [136], and bio-chemical hybrid processes, such as the bio-Fenton system (in which hydrogen peroxide is generated enzymatically in the presence of Fe^{2+} ions [137]) as well as photochemical and photocatalytic strategies utilizing specialized nanomaterials [41,132]. Beyond these approaches, the research group of P. Faria has systematically explored the ozonolysis of this dye under different reaction conditions and with various carbonaceous catalysts, such as activated carbon, both pure [42] and doped by various metal oxides [43,44]. The influence of activated carbon itself on the ozonation of AB 113 was confirmed in experiments using three different types of activated carbon: although no significant difference in color removal was observed, a pronounced decrease in TOC occurred in all cases when compared to the control (blank) experiment [42,44] (Table 4). In addition, different modifications of activated carbon such as acidic and basic activated carbon have been studied [44]. The influence of cerium oxide, activated carbon, and cerium-oxide-doped activated carbon was investigated in diluted (50 mg/L) AB 113 solutions. Under these conditions, adsorption onto activated carbon alone led to only minor color removal (18% after 2 h) [44]. In contrast, ozonation produced nearly complete decolorization within minutes—exceeding 90% within the first 10 min—even without any catalyst present [44]. The main problem of these experiments is the very slow decrease in TOC. Use of activated carbon, as a catalyst, definitely leads towards faster TOC removal [42–44]. Cerium oxide alone also promotes TOC reduction, albeit with a noticeable delay, with significant effects appearing only in the second hour of ozonation. Among the tested materials, the doped AC–CeOx catalyst exhibited the most pronounced TOC reduction [42,43].

Table 4. Comparison of AB113 ozonolysis using different carbon-based catalysts, with a summary comparing the decrease in absorbance (A) at 566 nm or Chemical Oxygen Demand (COD) and Total Organic Carbon (TOC).

Catalyst	Conc. [mg/L] and pH	Ozone Dose	Uncatalyzed Ozonation TOC/COD or Absorbance (A) Reduction Catalyzed Ozonation TOC/COD or Absorbance (A) Reduction	Lit.
Activated carbon	50–300 pH 7	2.15 mgO_3/min	A Decrease of 20% in **TOC** after 60 min (uncatal.) A decrease of 56% in **TOC** after 60 min	[42,44]
Activated carbon and ceria-doped activated carbon	50–300 pH 5.6	7.5 mgO_3/min	A decrease of 48% in **TOC** after 120 min (uncatal.) A decrease of 66% in **TOC** after 120 min (cat. by AC only) A decrease of 85% in **TOC** after 120 min (cat. by CeO_x-doped AC)	[42]
Cerium, manganese, and cobalt oxides supported on activated carbon	50–300 pH 5.5	7.5 mgO_3/min	A decrease of 45% in **TOC** after 120 min (uncatal.) A decrease of 72% in **TOC** after 120 min (cat. by AC only) A decrease of 74% in **TOC** after 120 min (cat. by MnO_x-doped AC) A decrease of 77% in **TOC** after 120 min (cat. by CoO_x-doped AC) A decrease of 88% in **TOC** after 120 min (cat. by CeO_x-doped AC)	[43]
Activated carbon	50 pH 7	0.5 mgO_3/min	A decrease of 17% in **TOC** after 300 min (uncatal.) A decrease of 60% in **TOC** after 300 min	[138]

Additional ozonation experiments using activated carbon doped with cobalt or manganese oxides likewise demonstrated an accelerated reaction compared to untreated activated carbon. Nevertheless, cerium-oxide-doped activated carbon again emerged as the most effective catalytic material for this dye [42,43].

5.4. Ozonolysis of Reactive Black 5

Another diazo dye, this time with an absorption maximum at 598 nm, is one of the most extensively studied textile dyes from the standpoint of available literature. Naturally, the effects of pH, ozone dosage, and other parameters on the course and kinetics of RB5 ozonization have been thoroughly studied [139–141]. In terms of carbonaceous material-catalyzed ozonolysis influence of powdered active carbon (PAC) [131], granulated active carbon (GAC) [51], carbon aerogel [50], ash [54], and bonechar material [49] have been studied. In several cases, carbonaceous materials have been doped by other catalytically active compounds (Table 5). From the values given in the table, it is possible to observe the direct influence of carbonaceous materials on the decomposition of ozone into hydroxyl radical, which is a well-known fact [142]. In addition, the data in Table 5 show that the decomposition proceeds much faster in a weakly alkaline environment. While in acidic and neutral environments oxidation occurs mainly through direct oxidation of the dye by ozone, in a weakly alkaline environment the decomposition of ozone into hydroxyl radical is preferred, which is an even stronger oxidizing agent than molecular ozone (the oxidation potential of ozone is 2.07 V while the oxidation potential of hydroxyl radical is 2.80 V). If we further raise the pH above 8 (pH $\geq$ 10), the recombination reaction between hydroxyl radicals will become more pronounced and the reaction rate will decrease [49,140]. Similar to the pH effect, the effect of doping a carbonaceous material with transition metal compounds can be observed in the case of ozonation of RB5 dye on GAC or Fe/Mn-doped GAC. Here, the effect of doping increased the efficiency of TOC reduction by almost 20%

under the same conditions, compared to the reaction catalyzed only by pure, undoped GAC [51].

Table 5. Comparison of RB5 ozonolysis using different carbon-based catalysts, with a summary comparing the decrease in absorbance (A) at 598 nm or Chemical Oxygen Demand (COD) and Total Organic Carbon (TOC).

Catalyst	Conc. [mg/L] and pH	Ozone Dose	Uncatalyzed Ozonation TOC/COD or Absorbance (A) Reduction Catalyzed Ozonation TOC/COD or Absorbance Reduction (A)	Lit.
-	100–500 pH 2–12	13–53 mgO_3/min	After 10 min of ozonation, 25–70% decrease in absorbance depending on ozone rate (uncatal.)	[140]
-	5 mg/L pH 7	16.44 or 24.66 mgO_3/min	**A** was removed by over 99% after 8 min (uncatal.).	[141]
PAC 149 µm	Approx. 800 pH 11.26	5 mgO_3/min	**A** was removed by over 90% after 30 min. **A** was removed by over 99% after 30 min.	[131]
Bonechar-doped ash doped with $MgO/Fe(NO_3)_2$	10–200 pH 2–10	**Not mentioned**	**Not mentioned** A decrease in **COD** of 60% after 30 min	[49]
Carbon aerogel doped by CuO	400–1600 pH 5.1	2–8 mgO_3/min	A decrease in **COD** (pH 5.1; c_{RB5} = 800 g/L; ozone dose: 4 mg/min) of 30% after 60 min A decrease in **COD** (pH 5.1; c_{RB5} = 800 g/L; ozone dose: 4 mg/min) of 45% after 60 min	[50]
GAC (granulated active carbon)	200 pH 7	3.3 mgO_3/min	**TOC** removal after 60 min: 32% **TOC** removal after minutes: 57%	[51]
Fe/Mn-doped GAC	200 pH 7	3.3 mgO_3/min	**TOC** removal after 60 min: 32% **TOC** removal after 60 min: 75%	[51]
Fe-dopped dead leaf ash	50 pH 2; 7; 9	1 gO_3/min	Not mentioned **A** was removed by 79 to 90% after 10 min, depending on catalyst dosage.	[54]

Ozonolysis of Reactive Black 5 in the present of other catalysts has been studied including the following: sonolysis [143], photocatalysis in the presence of a photocatalyst [144], UV-assisted decomposition of hydrogen peroxide into hydroxyl radicals and possible combinations of this approach with biological degradation [145], ozonolysis in the presence of nZVI [47], copper(II) sulfide [146], additives commonly used with these dyes such as sodium sulfate or sodium carbonate [147–150], and catalysis using doped zeolites [34]. For clarity, these methods are summarized in Table 6.

Table 6. Comparison of other catalysts used for RB5 ozonation.

Catalyst	Conc. [mg/L] and pH	Ozone Dose	Uncatalyzed Ozonation TOC/COD or Absorbance (A) Reduction Catalyzed Ozonation TOC/COD or Absorbance (A) Reduction	Lit.
Sonolysis	500 pH 5.7–12	50 mgO_3/min	**Not mentioned** **TOC** removal after 60 min: 57%	[143]
Photocat. TiO_2/UV	25–200 pH 5.4	**Not mentioned**	**TOC** removal after 100 min: 50% **TOC** removal just by UV irradiation in 100 min: over 60% **TOC** removal by irradiation in presence of a catalyst in 100 min: over 90%	[144]

Table 6. *Cont.*

Catalyst	Conc. [mg/L] and pH	Ozone Dose	Uncatalyzed Ozonation TOC/COD or Absorbance (A) Reduction Catalyzed Ozonation TOC/COD or Absorbance (A) Reduction	Lit.
Photocat. H_2O_2/UV	2100 pH 7	**Not mentioned**	**Not mentioned** After 560 min, over 90% of **DOC-dissolved organic carbon** was removed.	[145]
Pumices/nZVI (nano zero-valent iron)	50 pH 3–11	**Not mentioned**	**A** was removed by unmodified pumice (82%) after 60 min at pH 9 (uncatal.). **A** was removed by 99.8% after 60 min at pH 9.	[47]
CuS powder	100 pH 3; 7; 10	115 mgO_3/min	Approx. 75% **TOC** was removed after 80 min at pH 10 (uncatal.). Approx. 90% **TOC** was removed after 80 min at pH 10.	[146]
$CuMn_2O_4$-doped zeolite	30–1000 pH 3; 7.5; 10	0.75–1.5 mgO_3/min	**Not mentioned** (uncatal.) **A** was removed 90% (30 mg/L; 1,5 mgO_3/min) after 30 min.	[34]
H_2O_2/magnetic SiO_2/Fe_3O_4	50 pH 3–10	7.2–14.2 mgO_3/min	**TOC** removal after 60 min (uncatal.): 30% **TOC** removal after 60 min: 91%	[147]
Pyrite cinder/Ce^{3+}	200 pH 3–10	5.6 mgO_3/min	**TOC** removal after 120 min (uncatal.): 42% **TOC** removal after 120 min: 82%	[148]
Ag-Co oxide composite	100–1000 pH 2.2; 7; 10	30–60 L/hour O_2/O_3 mixture 1–3 gO_3/min	**A** was removed by > 90% after 20 min (uncatal.). **A** was removed by > 95% after 10 min. **TOC** was removed by over 95% (100 mg/L) after 80 min.	[36]
$CuMn_2O_4$/reduced graphene oxide-coated zeolites	30; 60; 90 pH 3; 7.5; 10	0.6–1.4 mgO_3/min	**A** was removed by 77–84% after 30 min (uncatal.). **A** was removed by 87–94% after 30 min.	[37]
Ag-Ce oxides composite	100–500 pH 2; 7; 10	30–60 L/hour O_2/O_3 mixture 1–3 gO_3/min	**A** was removed by > 90% after 20 min (uncatal.). **A** was removed by > 95% after 10 min. A 88% decrease in **COD** after 80 min	[38]
Mn-Ce oxide-loaded Al_2O_3	300 pH 3–11	2.1 mgO_3/min	A 30% decrease in **COD** after 60 min (uncatal.) A 60% decrease in **COD** after 60 min	[39]

All these studies show that although the decolorization of RB5 solutions occurs within minutes of ozonation even without a catalyst, the real challenge lies in the removal of TOC and COD, which—logically—proceeds more slowly. This is where catalytic ozonation becomes important. All catalytic ozonations listed in Tables 5 and 6 show a more pronounced decrease in TOC or COD compared to the blank experiment, highlighting the potential usefulness of ozonation catalysts. The optimal pH for most of these ozonizations was found to be in the alkaline range (pH 10–11), which corresponds to the well-known behavior of ozone decomposition in water at elevated pH [142].

From an economic point of view, the possible cost of using these carbon-based catalysts and other catalysts is significant. Section 2 discusses the production of carbonaceous materials from more or less waste plant materials, which can subsequently be used as catalysts for ozonation reactions. Given that these materials are most often doped with common transition and non-transition metals (Mg, Fe, Mn, etc.) [49,51,54], the price of these materials is significantly lower than complicated catalysts based on more expensive elements (such as Ce, Cu, Co, or Ag), or nanoparticles and other materials with more complicated preparation/production on a large scale.

Likewise, thanks to doping metals such as Fe, Mn, or Mg [49,51,54], which do not pose such a problem in the event of release into the environment as in the case of materials doped with copper, cobalt, or silver, i.e., elements with a generally known antimicrobial effect which are also toxic to the aquatic environment. In the case of nanomaterials, their toxicology is so complicated that it far exceeds the possibilities of discussion in this publication.

Thanks to experiments by Bilińska, Zheng, and Wang, we now have a relatively good knowledge of the ozonation process of the azo dye Reactive Black 5 (Scheme 13). This theoretical ozonation reaction pathway is based on GC-MS/HPLC-MS measurements of the product mixture [131,140,151].

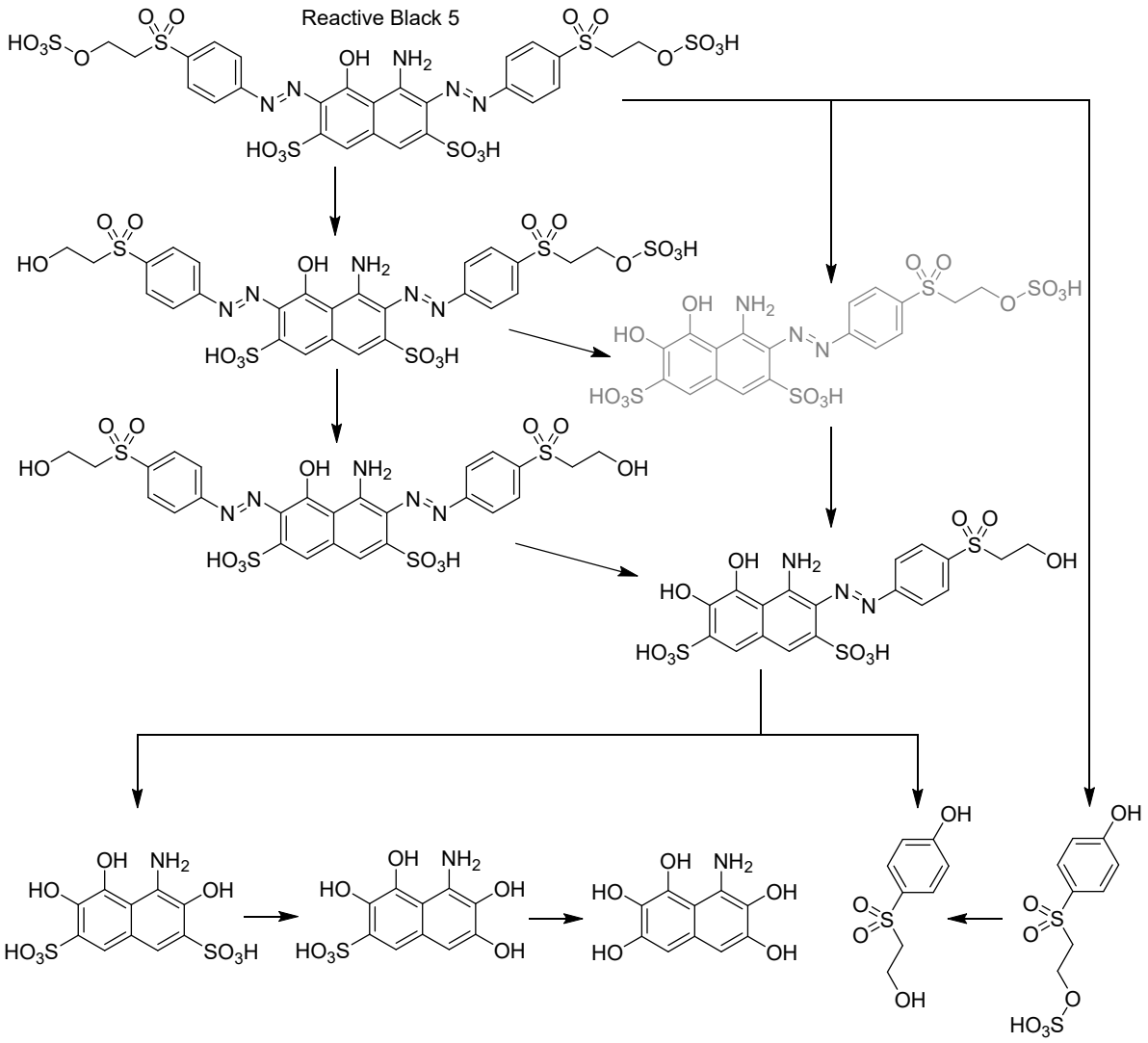

Scheme 13. Proposed ozonation reaction pathway of RB5 ozonation by Bilińska. The grey-colored compound was not identified by LC-MS [140].

In the case of a possible process of dye decomposition, it can be seen from the analyses performed that the most susceptible groups for oxidation by ozone/hydroxyl radical are sulfo groups and groups derived from sulfonic acid (R-SO_2-R). These reactions are summarized in Schemes 13 and 14 and especially Scheme 15, where partial reactions of oxidation by ozone under catalysis by carbonaceous materials are presented [131,140,152–154].

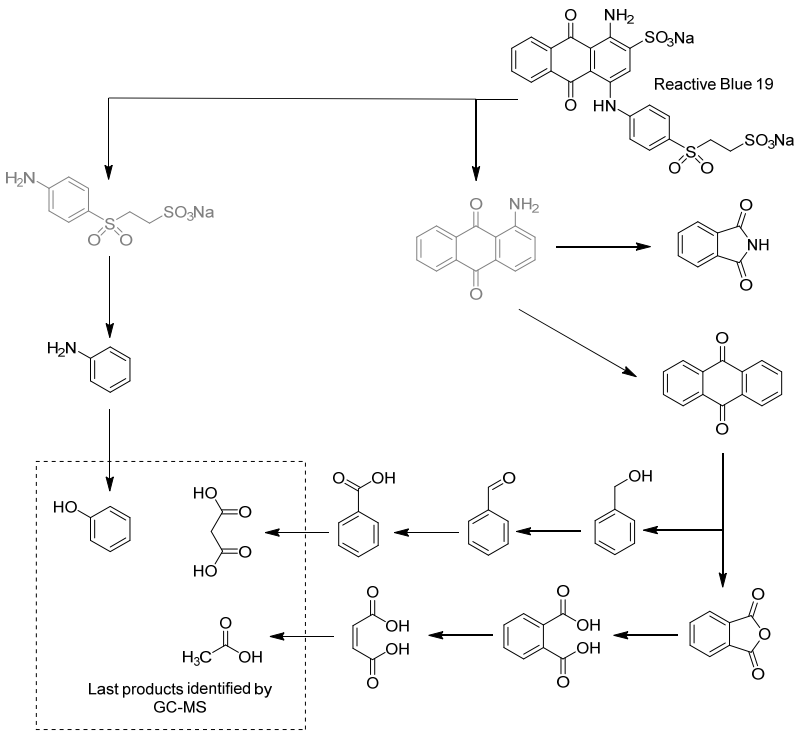

Scheme 14. RB19 ozonation degradation pathway by Lovato, based on GC-MS measurement. The grey compounds have not been identified by GC-MS [154].

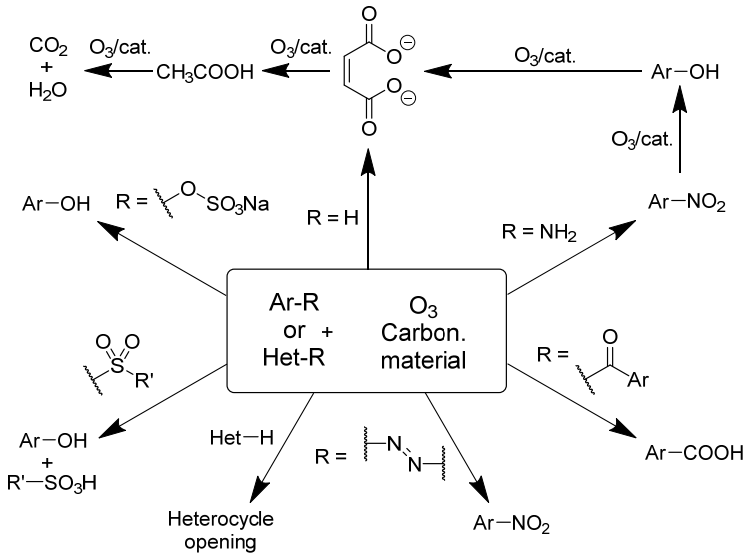

Scheme 15. Reactivity of different substrates towards O_3 in the presence of carbonaceous materials.

5.5. Ozonolysis of Reactive Blue 19

This anthraquinone dye, with an absorption maximum at 592 nm, has been studied using a variety of degradation approaches, including photocatalytic [152] and biological processes (achieving up to 90% removal within 24 h [153]). Although the biological removal data appear encouraging, the method proves ineffective at higher dye concentrations: above 400 mg/L the decolorization slows considerably, and at 1 g/L virtually, no decolorization occurs [153]).

Consequently, ozonation—particularly in combination with catalysts—remains an attractive strategy for the degradation of this dye. Simple ozonation alone can achieve a 100% reduction in absorbance at 592 nm within 10 min [154]. Moreover, experiments

indicate improved degradation under alkaline conditions (showing roughly a 5% enhancement at pH 10 compared to at pH 6.5), a finding corroborated by other RB19 ozonation studies [139,155]. Under these conditions, COD decreased by 55% after 90 min, and TOC fell by 17% (COD_0 = 784 mg O_2/L, TOC_0 = 229 mg/L) [155].

Among ozonation modifications for RB19, sonolysis stands out: at a dye concentration of 30 mg/L, the application of 120 W/L ultrasound produced nearly a 1.5-fold acceleration in decolorization rate relative to the control [156].

Another example is the enhancement achieved using calcium peroxide, where dye solutions ranging from 5 to 300 mg/L exhibited significantly higher degradation efficiencies than with ozonation alone [157].

True catalytic ozonation is achieved using carbon aerogel or its Co_3O_4-doped analogue. In this system, not only was 95% decolorization achieved within 5 min for wastewater taken directly from dye baths (including Na_2CO_3 and other additives), but an 80% decrease in COD was observed after only 30 min—approximately 30% higher than in the non-catalyzed ozonation of the same wastewater [40] (Table 7).

Table 7. Methods used for ozonolysis of RB19, with a summary comparing the decrease in absorbance (A) at 592 nm or Chemical Oxygen Demand (COD) and Total Organic Carbon (TOC).

Catalyst	Conc. [mg/L] and pH	Ozone Dose	Uncatalyzed Ozonation TOC/COD or Absorbance (A) Reduction Catalyzed Ozonation TOC/COD or Absorbance (A) Reduction	Lit.
-	111–466 pH 3–10	56–91 mgO_3/min	A 52% **TOC** removal after 120 min at an O_3 dose of 56 mgO_3/min (uncatal.) A 66% **TOC** removal after 120 min at an O_3 dose of 71 mgO_3/min (uncatal.) An 86% **TOC** removal after 120 min at an O_3 dose of 91 mgO_3/min (uncatal.)	[154]
-	100–800 pH 7	4.4 mgO_3/min	A 17% **TOC** removal after 90 min of ozonation (800 mg/L) (uncatal.)	[155]
Sonolysis	30–100 mg/L pH 5.5; 11	4.6–9.4 mgO_3/L	A decrease of 88% in **A** (100 mg/L, ozone concentration: 9.4 mg/L) after 13 min (uncatal.) A decrease of 99% in **A** (100 mg/L, ozone concentration: 9.4 mg/L, 120 W/L ultrasound) after 13 min	[156]
Carbon aerogel	Exact concentration not mentioned. pH > 10	2.5 mgO_3/min	An approx. 50% decrease in **COD** after 30 min (uncatal.) An approx. 65% decrease in **COD** after 30 min	[40]
Co_3O_4 doped carbon aerogel	Exact concentration not mentioned pH > 10	2.5 mgO_3/min	An approx. 50% decrease in **COD** after 30 min (uncatal.) An approx. 80% decrease in **COD** after 30 min	[40]
Calcium peroxide cat. (0–0.1 g CaO_2)	5–300 pH 3–11	1 gO_3/min	**Not mentioned** (uncatal.) A removal of 85.6% of **COD** after 50 min at pH = 3	[157]
Homocatalysis by TAED (tetraacetyl-ethylenediamine)	100 pH 4–10	0.5–8.5 mgO_3/min	A 64% decrease in **A** (uncatal.) A 90% decrease in **A** (0.025 g/L TAED)	[130]

Thanks to Lovato et al. who used GC-MS to analyze the product mixture, we now have a fairly good understanding of the composition of the RB19 ozonolysis product mixture,

and thanks to changes in this composition over time, we can estimate the likely ozonation pathways [154] (Scheme 14).

5.6. Ozonolysis of Reactive Red 198

The azo dye RR198 exhibits an absorption maximum at 518 nm. Although ozonation has been studied, it is not the predominant method for degrading RR198; photocatalytic processes involving TiO_2 [133] and its doped derivatives [158], graphene oxide [159], and various biodegradation routes [160,161] are more frequently reported. UV-assisted ozonation further demonstrated the synergistic interaction between UV irradiation and ozone [162].

Within ozonation research, the influence of pH and ozone dosage has been examined for solutions at 100, 250, and 500 mg/L, which underwent decolorization after 10, 25, and 60 min, respectively, depending on the starting concentration. For a 250 mg/L solution at pH 10, a 60% reduction in COD was achieved within one hour [163].

Only two articles were found describing the ozonation of RR198 catalyzed by carbon-based materials [52,53]. In the first study, MWCNTs (multiwalled carbon nanotubes) were employed in a photocatalytic ozonation system. It was shown that MWCNTs on their own exhibit no catalytic activity in the absence of UV irradiation; however, under UV-assisted photocatalysis, MWCNTs significantly accelerated the decline in absorbance of the ozonized solution. The study also examined the influence of common dyeing additives such as Na_2CO_3 and $NaHCO_3$, both of which clearly inhibited the ozonation rate [52]. In the second study, biochar produced from pistachio shells at 500 °C was used as a catalyst. Using a biochar dosage of 2 g/L and an RR198 concentration of 100 mg/L, the material exhibited strong catalytic activity: after 10 min of ozonation, absorbance decreased by 65% at pH 3 and by 84% at pH 10, whereas non-catalyzed ozonation achieved less than a 20% reduction in the same period. A comparison was also made with commercially available activated carbon. In this head-to-head comparison, the prepared biochar outperformed activated carbon by a wide margin, achieving more than 95% degradation of RR198, while activated carbon reached only about 40% after one hour of ozonation [53] (Table 8).

Table 8. Catalysts used for ozonolysis of RR198.

Catalyst	Conc. [mg/L] and pH	Ozone Dose	Uncatalyzed Ozonation TOC/COD or Absorbance (A) Reduction Catalyzed Ozonation TOC/COD or Absorbance (A) Reduction	Lit.
-	66–200 Dye mixture pH 3.6–10.4	80 mgO_3/min	A 53% **COD** removal after 30 min (200 mg/L, pH 9) (uncatal.) A 55% **COD** removal after 30 min (100 mg/L, pH 9) (uncatal.) A 67% **COD** removal after 30 min (100 mg/L, pH 5) (uncatal.)	[164]
Activated carbon or biochar	100 pH 10	1.5 mgO_3/min	An approx. 20% **A** removal after 60 min (uncatal.) An approx. 40% **A** removal after 60 min of ozonation with activated carbon An over 90% **A** removal after 60 min of ozonation with biochar A 71% **TOC** removal after 60 min of ozonation with biochar	[53]
Multiwalled carbon nanotubes (MWCNTs)	50–200 pH 3–7	2.5 mgO_3/min	An approx. 80% **A** removal after 12 min without a catalyst An over 95% **A** removal after 12 min of ozonation with MWCNTs—faster mineralization	[52]
UV	50–300 pH 5 < pH < 9	40 mgO_3/min	An approx. 53% decrease in **TOC** after 60 min (50 mg/L) (uncatal.) An approx. 76% decrease in **TOC** after 60 min (50 mg/L, UV)	[162]
MgO nanocrystals	100–500 pH 2–12	3.33 mgO_3/min	An approx. 30% decrease in **COD** after 20 min (200 mg/L, pH 8) (uncatal.) An approx. 60% decrease in **COD** after 20 min (200 mg/L, pH 8)	[53]
TiO_2/UV	100–200 pH 4; 7; 10	1.83 mgO_3/min	An approx. 40% **A** removal after 60 min without a catalyst (uncatal.) An approx. 52% **A** removal after 60 min without a catalyst	[165]

The above-mentioned ozonation processes (Scheme 15) documented effect of different carbon-based catalysts in comparison with other catalytic systems. However, carbon-based

materials are characterized by the relatively low price, sorption ability for persistent organic contaminants, and catalytic effect in ozonation processes.

Although all these reactions play a role in the decomposition of dyes (Schemes 13 and 14) and also drugs (see Scheme 11—decomposition of sulfathiazole), it is more than obvious that the functional groups most easily reacting with ozone and hydroxyl radical are sulfonic acids and functional groups derived from them, which usually decompose into alcohols, while the rest of the sulfo group can then be oxidized to inorganic sulfates. Other possibilities are the oxidation of amines to nitro compounds, followed by their subsequent oxidation to alcohols/phenols with the simultaneous release of nitrogen oxides. Azo bonds also undergo oxidation to form nitro compounds, which are further oxidized to the aforementioned phenols [14,140,154].

6. Conclusions

This review would like to denote possible utilization of simply industrially available materials such as active carbon or biochar for degradation of persistent pollutants in contaminated aqueous solutions.

This paper describes the methods and applications of carbonaceous catalysts for ozone-based advanced oxidation processes. The catalytic effects of different types of carbonaceous materials such as active carbon and biochar were compared in ozonation of drugs and textile dyestuffs.

Although the application of biochar for ozonation processes show great potential as catalysts for oxidative removal of persistent contaminants from wastewater, its application on an industrial scale still faces several techno-economic and environmental challenges.

One of the main challenges is the wide variability in biochar properties, depending on the biomass type and pyrolysis conditions. These factors could lead to non-uniformity in catalytic performance. Consistency and reproducibility of the carbonaceous material are important issues in its industrial application.

In addition, most studies are still at the laboratory level, so the scale-up of biochar production processes and catalytic applications in real ozone-based water treatment systems have not been tested practically.

Another issue is the long-term catalytic efficiency of applied biochar. The gradual surface oxidation of applied biochar generally could influence the catalytic performance of these materials causing significant changes in specific surface area.

From an economic point of view, the average price of active carbon is US $20/kg [166].

Biochar seems to be an interesting carbon-based catalyst since biochar is derived from inexpensive biomass waste (approximately US $0.025/kg for rice husk [167]. On the other hand, necessary pyrolytic (or even modification) processes could significantly increase the production costs of biochar. Still, the price of biochar (ca. US $5–10/kg) even after modification is much lower than the price of carbon materials commonly used in industry [167].

The strength of this review is its predominant focus on environmentally benign carbonaceous catalysts such as active carbon or biochar, providing a broad perspective on their practical potential and limitations in ozonation processes [168] or even in ozonation processes combined with subsequent biological treatment [169,170]

However, a limitation of this article lies in the variability of experimental conditions across the studies discussed, which can complicate direct comparisons of ozonation efficiencies and operational performance.

Nonetheless, this review serves as a valuable reference for researchers seeking sustainable solutions for effective oxidative treatment of drug- or dye-contaminated wastewaters.

Author Contributions: P.L., J.M., and T.W. conceived, designed and wrote the paper. All authors have read and agreed to the published version of the manuscript.

Funding: This research received no external funding.

Data Availability Statement: No new data were created or analyzed in this study. Data sharing is not applicable to this article.

Acknowledgments: This work was supported by the Faculty of Chemical Technology, University of Pardubice.

Conflicts of Interest: The authors declare no conflicts of interest.

References

1. Godiya, C.B.; Leiviskä, T. Wood-Derived Adsorbents for the Removal of Pharmaceutical Contamination from Wastewater: A Review. *Environ. Chem. Lett.* **2025**, *23*, 1–31. [CrossRef]
2. Paździor, K.; Bilińska, L.; Ledakowicz, S. A Review of the Existing and Emerging Technologies in the Combination of AOPs and Biological Processes in Industrial Textile Wastewater Treatment. *Chem. Eng. J.* **2019**, *376*, 120597. [CrossRef]
3. Ahmed, H.R.; Ealias, A.M.; George, G. Advanced Oxidation Processes for the Removal of Antidepressants from Wastewater: A Comprehensive Review. *RSC Adv.* **2025**, *15*, 48639–48665. [CrossRef]
4. Alrefaey, K.A.; Sallam, N.A.; ElZayat, E.M.; Youssef, A.F.A.; Fahim, I.S.; Hosney, H.; Lens, P.N.L. A Comprehensive Review of Techniques for Removal of Antibiotics from Wastewater. *Environ. Sci. Water Res. Technol.* **2025**, *11*, 2782–2809. [CrossRef]
5. Yang, X.; Zhang, T.; Liu, Z.; Zhang, R.; Chen, C.; Li, Z.; Demeestere, K.; Van Hulle, S.W.H. Intensification of Ozone Gas/Liquid Mass Transfer and Ozonation Efficiency: A Critical Review. *Water Res.* **2026**, *288*, 124719. [CrossRef]
6. Buffle, M.-O.; Schumacher, J.; Salhi, E.; Jekel, M.; von Gunten, U. Measurement of the Initial Phase of Ozone Decomposition in Water and Wastewater by Means of a Continuous Quench-Flow System: Application to Disinfection and Pharmaceutical Oxidation. *Water Res.* **2006**, *40*, 1884–1894. [CrossRef]
7. Nemr, A.E.; Hassaan, M.A.; Madkour, F.F. HPLC-MS/MS Mechanistic Study of Direct Yellow 12 Dye Degradation Using Ultraviolet Assisted Ozone Process. *J. Water Environ. Nanotechnol.* **2018**, *3*, 1–11. [CrossRef]
8. Wang, J.; Chen, H. Catalytic ozonation for water and wastewater treatment: Recent advances and perspective. *Sci. Total Environ.* **2020**, *704*, 135249. [CrossRef]
9. Nemati Sani, O.; Navaei fezabady, A.A.; Yazdani, M.; Taghavi, M. Catalytic Ozonation of Ciprofloxacin Using γ-Al_2O_3 Nanoparticles in Synthetic and Real Wastewaters. *J. Water Process Eng.* **2019**, *32*, 100894. [CrossRef]
10. Liu, H.; Gao, Y.; Wang, J.; Pan, J.; Gao, B.; Yue, Q. Catalytic Ozonation Performance and Mechanism of Mn-CeOx@γ-Al_2O_3/O_3 in the Treatment of Sulfate-Containing Hypersaline Antibiotic Wastewater. *Sci. Total Environ.* **2022**, *807*, 150867. [CrossRef]
11. Noman, M.; Yu, G.; Tsegaye Awugichew, D.; Li, X. Synthesis of Surficial-Modified Green Biochar Catalyst Generated by Biogas Residue Biochar and Potential Application for Catalytic Ozonation Degradation of Ciprofloxacin. *Environ. Res.* **2024**, *257*, 119314. [CrossRef]
12. Sui, M.; Xing, S.; Sheng, L.; Huang, S.; Guo, H. Heterogeneous Catalytic Ozonation of Ciprofloxacin in Water with Carbon Nanotube Supported Manganese Oxides as Catalyst. *J. Hazard. Mater.* **2012**, *227–228*, 227–236. [CrossRef] [PubMed]
13. Szabová, P.; Hencelová, K.; Sameliaková, Z.; Marcová, T.; Staňová, A.V.; Grabicová, K.; Bodík, I. Ozonation: Effective Way for Removal of Pharmaceuticals from Wastewater. *Monatshefte Für Chem. Chem. Mon.* **2020**, *151*, 685–691. [CrossRef]
14. Adamek, E.; Baran, W. Degradation of Veterinary Antibiotics by the Ozonation Process: Product Identification and Ecotoxicity Assessment. *J. Hazard. Mater.* **2024**, *469*, 134026. [CrossRef]
15. Rekhate, C.V.; Srivastava, J.K. Recent advances in ozone-based advanced oxidation processes for treatment of wastewater—A review. *Chem. Eng. J. Advances* **2020**, *3*, 100031. [CrossRef]
16. Tahergorabi, M.; Esrafili, A.; Kermani, M.; Gholami, M.; Farzadkia, M. Degradation of Four Antibiotics from Aqueous Solution by Ozonation: Intermediates Identification and Reaction Pathways. *Desalination Water Treat.* **2019**, *139*, 277–287. [CrossRef]
17. Dawood, F.K.; Abdulrazzaq, N.N. Direct Oxidation of Antibiotics from Aqueous Solution by Ozonation with Microbubbles. *J. Phys. Conf. Ser.* **2021**, *1973*, 012157. [CrossRef]
18. Yargeau, V.; Leclair, C. Impact of Operating Conditions on Decomposition of Antibiotics During Ozonation: A Review. *Ozone Sci. Eng.* **2008**, *30*, 175–188. [CrossRef]
19. Biń, A.K.; Sobera-Madej, S. Comparison of the Advanced Oxidation Processes (UV, UV/H_2O_2 and O_3) for the Removal of Antibiotic Substances during Wastewater Treatment. *Ozone Sci. Eng.* **2012**, *34*, 136–139. [CrossRef]
20. Kudlek, E.; Dudziak, M. Toxicity and Degradation Pathways of Selected Micropollutants in Water Solutions during the O_3 and O_3/H_2O_2 Process. *Desalination Water Treat.* **2018**, *117*, 88–100. [CrossRef]

21. Lu, J.; Sun, Q.; Wu, J.; Zhu, G. Enhanced Ozonation of Antibiotics Using Magnetic $Mg(OH)_2$ Nanoparticles Made through Magnesium Recovery from Discarded Bischofite. *Chemosphere* **2020**, *238*, 124694. [CrossRef]
22. Oncu, N.B.; Balcioglu, I.A. Degradation of Ciprofloxacin and Oxytetracycline Antibiotics in Waste Sewage Sludge by Ozonation. *J. Adv. Oxid. Technol.* **2013**, *16*, 107–116. [CrossRef]
23. Verinda, S.B.; Muniroh, M.; Yulianto, E.; Maharani, N.; Gunawan, G.; Amalia, N.F.; Hobley, J.; Usman, A.; Nur, M. Degradation of Ciprofloxacin in Aqueous Solution Using Ozone Microbubbles: Spectroscopic, Kinetics, and Antibacterial Analysis. *Heliyon* **2022**, *8*, e10137. [CrossRef]
24. Ivantsova, N.A.; Karataeva, P.R. Catalytic Ozonation of Aqueous Solution of Paracetamol. *Russ. J. Gen. Chem.* **2022**, *92*, 3020–3024. [CrossRef]
25. Gotvajn, A.Ž.; Rozman, U.; Antončič, T.; Urbanc, T.; Vrabeľ, M.; Derco, J. Fe^{2+} and UV Catalytically Enhanced Ozonation of Selected Environmentally Persistent Antibiotics. *Processes* **2021**, *9*, 521. [CrossRef]
26. Qiu, J.-L.; Li, D.-W.; Jing, S.-C.; Qiu, H.; Liu, F.-Q. Advanced technique of catalytic ozonation-enhanced coagulation for the efficient removal of low coagulability refractory organics from secondary effluent. *Chemosphere* **2022**, *303*, 135157. [CrossRef]
27. Beltrán, F.J.; Pocostales, P.; Alvarez, P.; Oropesa, A. Diclofenac Removal from Water with Ozone and Activated Carbon. *J. Hazard. Mater.* **2009**, *163*, 768–776. [CrossRef]
28. Gonçalves, A.G.; Órfão, J.J.M.; Pereira, M.F.R. Ozonation of Erythromycin over Carbon Materials and Ceria Dispersed on Carbon Materials. *Chem. Eng. J.* **2014**, *250*, 366–376. [CrossRef]
29. Orge, C.A.; Graça, C.A.L.; Restivo, J.; Pereira, M.F.R.; Soares, O.S.G.P. Catalytic Ozonation of Pharmaceutical Compounds Using Carbon-Based Catalysts. *Catal. Commun.* **2024**, *187*, 106863. [CrossRef]
30. Moreira, N.F.F.; Orge, C.A.; Ribeiro, A.R.; Faria, J.L.; Nunes, O.C.; Pereira, M.F.R.; Silva, A.M.T. Fast Mineralization and Detoxification of Amoxicillin and Diclofenac by Photocatalytic Ozonation and Application to an Urban Wastewater. *Water Res.* **2015**, *87*, 87–96. [CrossRef]
31. Somensi, C.A.; Souza, A.L.F.; Simionatto, E.L.; Gaspareto, P.; Millet, M.; Radetski, C.M. Genetic Material Present in Hospital Wastewaters: Evaluation of the Efficiency of DNA Denaturation by Ozonolysis and Ozonolysis/Sonolysis Treatments. *J. Environ. Manag.* **2015**, *162*, 74–80. [CrossRef]
32. Crousier, C.; Pic, J.-S.; Albet, J.; Baig, S.; Roustan, M. Urban Wastewater Treatment by Catalytic Ozonation. *Ozone Sci. Eng.* **2015**, *38*, 3–13. [CrossRef]
33. He, S.; Li, J.; Xu, J.; Mo, L.; Zhu, L.; Luan, P.; Zeng, J. Heterogeneous Catalytic Ozonation of Paper-Making Wastewater with α-Fe_2O_3/γ-Al_2O_3 as a Catalyst for Increased TOC and Color Removals. *Desalination Water Treat.* **2017**, *95*, 192–199. [CrossRef]
34. Ikhlaq, A.; Zafar, M.; Javed, F.; Yasar, A.; Akram, A.; Shabbir, S.; Qi, F. Catalytic Ozonation for the Removal of Reactive Black 5 (RB-5) Dye Using Zeolites Modified with $CuMn_2O_4/gC_3N_4$ in a Synergic Electro Flocculation-Catalytic Ozonation Process. *Water Sci. Technol.* **2021**, *84*, 1943–1953. [CrossRef]
35. Saleh, I.A.; Zouari, N.; Al-Ghouti, M.A. Removal of pesticides from water and wastewater: Chemical, physical and biological treatment approaches. *Environ. Technol. Innov.* **2020**, *19*, 101026. [CrossRef]
36. Chokshi, N.P.; Ruparelia, J.P. Catalytic Ozonation of Reactive Black 5 over Silver–Cobalt Composite Oxide Catalyst. *J. Inst. Eng. Ser. A* **2020**, *101*, 433–443. [CrossRef]
37. Ikhlaq, A.; Shabbir, S.; Javed, F.; Kazmi, M.; Yasir, A.; Qazi, U.Y.; Zafar, M.; Qi, F. Catalytic Ozonation Combined Electroflocculation for the Removal of Reactive Black 5 in Aqueous Solution Using $CuMn_2O_4$/RGO Coated Zeolites. *Desalination Water Treat.* **2022**, *259*, 221–229. [CrossRef]
38. Chokshi, N.P.; Chauhan, A.; Chhayani, R.; Sharma, S.; Ruparelia, J.P. Preparation and Application of Ag–Ce–O Composite Metal Oxide Catalyst in Catalytic Ozonation for Elimination of Reactive Black 5 Dye from Aqueous Media. *Water Sci. Eng.* **2024**, *17*, 257–265. [CrossRef]
39. Li, S.; Li, W.; Wu, Y.; Zheng, X.; Zhao, X.; Nan, N.; Zhang, H. Preparation of Mn-Ce Oxide-Loaded Al_2O_3 by Citric Acid-Assisted Impregnation for Enhanced Catalytic Ozonation Degradation of Dye Wastewater. *Chin. J. Chem. Eng.* **2024**, *76*, 237–250. [CrossRef]
40. Hu, E.; Shang, S.; Tao, X.; Jiang, S.; Chiu, K. Regeneration and Reuse of Highly Polluting Textile Dyeing Effluents through Catalytic Ozonation with Carbon Aerogel Catalysts. *J. Clean. Prod.* **2016**, *137*, 1055–1065. [CrossRef]
41. Suganya Josephine, G.A.; Mary Nisha, U.; Meenakshi, G.; Sivasamy, A. Nanocrystalline Semiconductor Doped Rare Earth Oxide for the Photocatalytic Degradation Studies on Acid Blue 113: A Di-Azo Compound under UV Slurry Photoreactor. *Ecotoxicol. Environ. Saf.* **2015**, *121*, 67–72. [CrossRef]
42. Faria, P.C.C.; Órfão, J.J.M.; Pereira, M.F.R. Activated Carbon and Ceria Catalysts Applied to the Catalytic Ozonation of Dyes and Textile Effluents. *Appl. Catal. B Environ.* **2009**, *88*, 341–350. [CrossRef]
43. Faria, P.C.C.; Monteiro, D.C.M.; Órfão, J.J.M.; Pereira, M.F.R. Cerium, Manganese and Cobalt Oxides as Catalysts for the Ozonation of Selected Organic Compounds. *Chemosphere* **2009**, *74*, 818–824. [CrossRef] [PubMed]
44. Faria, P.C.C.; Órfão, J.J.M.; Pereira, M.F.R. Mineralisation of Coloured Aqueous Solutions by Ozonation in the Presence of Activated Carbon. *Water Res.* **2005**, *39*, 1461–1470. [CrossRef]

45. Xiang, Z.; Zhang, Y.; Bo, L.; Shen, Z.; Wang, D.; Shen, Z.; Tang, Y. Removal Performance and Mechanism of Aniline from Landfill Leachate by Ozone Oxidation Process Using Iron-Based Packed Catalyst. *J. Environ. Manag.* **2025**, *375*, 124397. [CrossRef] [PubMed]
46. Malik, S.N.; Khan, S.M.; Ghosh, P.C.; Vaidya, A.N.; Das, S.; Mudliar, S.N. Nano Catalytic Ozonation of Biomethanated Distillery Wastewater for Biodegradability Enhancement, Color and Toxicity Reduction with Biofuel Production. *Chemosphere* **2019**, *230*, 449–461. [CrossRef]
47. Rahmani, A.; Rahmani, H.; Rahmani, K. Degradation Reactive Black 5 Dye from Aqueous Solutions Using Ozonation with Pumices and Pumices Modified by Nanoscale Zero Valent Iron (nZVI). *Glob. NEST J.* **2020**, *22*, 336–341. [CrossRef]
48. Zimmermann, S.G.; Wittenwiler, M.; Hollender, J.; Krauss, M.; Ort, C.; Siegrist, H.; von Gunten, U. Kinetic Assessment and Modeling of an Ozonation Step for Full-Scale Municipal Wastewater Treatment: Micropollutant Oxidation, by-Product Formation and Disinfection. *Water Res.* **2011**, *45*, 605–617. [CrossRef]
49. Asgari, G.; Akbari, S.; Mohammadi, A.M.S.; Poormohammadi, A.; Ramavandi, B. Preparation and Catalytic Activity of Bone-Char Ash Decorated with MgO-$FeNO_3$ for Ozonation of Reactive Black 5 Dye from Aqueous Solution: Taguchi Optimization Data. *Data Brief* **2017**, *13*, 132–136. [CrossRef]
50. Hu, E.; Wu, X.; Shang, S.; Tao, X.; Jiang, S.; Gan, L. Catalytic Ozonation of Simulated Textile Dyeing Wastewater Using Mesoporous Carbon Aerogel Supported Copper Oxide Catalyst. *J. Clean. Prod.* **2016**, *112*, 4710–4718. [CrossRef]
51. He, H.; Wu, D.; Lv, Y.; Ma, L. Enhanced Mineralization of Aqueous Reactive Black 5 by Catalytic Ozonation in the Presence of Modified GAC. *Desalination Water Treat.* **2016**, *57*, 14997–15006. [CrossRef]
52. Mahmoodi, N.M. Photocatalytic Ozonation of Dyes Using Multiwalled Carbon Nanotube. *J. Mol. Catal. A Chem.* **2013**, *366*, 254–260. [CrossRef]
53. Moussavi, G.; Khosravi, R. Preparation and Characterization of a Biochar from Pistachio Hull Biomass and Its Catalytic Potential for Ozonation of Water Recalcitrant Contaminants. *Bioresour. Technol.* **2012**, *119*, 66–71. [CrossRef]
54. Hussain, L.; Javed, F.; Tahir, M.W.; Munir, H.M.S.; Ikhlaq, A.; Wołowicz, A. Catalytic Ozonation of Reactive Black 5 in Aqueous Solution Using Iron-Loaded Dead Leaf Ash for Wastewater Remediation. *Molecules* **2024**, *29*, 836. [CrossRef]
55. Bilińska, L.; Blus, K.; Bilińska, M.; Gmurek, M. Industrial Textile Wastewater Ozone Treatment: Catalyst Selection. *Catalysts* **2020**, *10*, 611. [CrossRef]
56. Hama Aziz, K.H.; Mustafa, F.S.; Karim, M.A.H.; Hama, S. Biochar-Based Catalysts: An Efficient and Sustainable Approach for Water Remediation from Organic Pollutants via Advanced Oxidation Processes. *J. Environ. Manag.* **2025**, *390*, 126245. [CrossRef] [PubMed]
57. Nowak, M.; Czekała, W. Sustainable Use of Digestate from Biogas Plants: Separation of Raw Digestate and Liquid Fraction Processing. *Sustainability* **2024**, *16*, 5461. [CrossRef]
58. Zhang, Z.; Zhu, Z.; Shen, B.; Liu, L. Insights into Biochar and Hydrochar Production and Applications: A Review. *Energy* **2019**, *171*, 581–598. [CrossRef]
59. Khan, S.; Irshad, S.; Mehmood, K.; Hasnain, Z.; Nawaz, M.; Rais, A.; Gul, S.; Wahid, M.A.; Hashem, A.; Abd_Allah, E.F.; et al. Biochar Production and Characteristics, Its Impacts on Soil Health, Crop Production, and Yield Enhancement: A Review. *Plants* **2024**, *13*, 166. [CrossRef]
60. Seow, Y.X.; Tan, Y.H.; Mubarak, N.M.; Kansedo, J.; Khalid, M.; Ibrahim, M.L.; Ghasemi, M. A Review on Biochar Production from Different Biomass Wastes by Recent Carbonization Technologies and Its Sustainable Applications. *J. Environ. Chem. Eng.* **2022**, *10*, 107017. [CrossRef]
61. Sharma, T.; Hakeem, I.G.; Gupta, A.B.; Joshi, J.; Shah, K.; Vuppaladadiyam, A.K.; Sharma, A. Parametric Influence of Process Conditions on Thermochemical Techniques for Biochar Production: A State-of-the-Art Review. *J. Energy Inst.* **2024**, *113*, 101559. [CrossRef]
62. Kamarudin, N.S.; Dahalan, F.A.; Hasan, M.; An, O.S.; Parmin, N.A.; Ibrahim, N.; Hamdzah, M.; Zain, N.A.M.; Muda, K.; Wikurendra, E.A. Biochar: A Review of Its History, Characteristics, Factors That Influence Its Yield, Methods of Production, Application in Wastewater Treatment and Recent Development. *Biointerface Res. Appl. Chem.* **2021**, *12*, 7914–7926. [CrossRef]
63. Hagemann, N.; Spokas, K.; Schmidt, H.-P.; Kägi, R.; Böhler, M.; Bucheli, T. Activated Carbon, Biochar and Charcoal: Linkages and Synergies across Pyrogenic Carbon's ABCs. *Water* **2018**, *10*, 182. [CrossRef]
64. Alhashimi, H.A.; Aktas, C.B. Life Cycle Environmental and Economic Performance of Biochar Compared with Activated Carbon: A Meta-Analysis. *Resour. Conserv. Recycl.* **2017**, *118*, 13–26. [CrossRef]
65. Shaheen, J.; Fseha, Y.H.; Sizirici, B. Performance, Life Cycle Assessment, and Economic Comparison between Date Palm Waste Biochar and Activated Carbon Derived from Woody Biomass. *Heliyon* **2022**, *8*, e12388. [CrossRef] [PubMed]
66. Kazemi Shariat Panahi, H.; Dehhaghi, M.; Ok, Y.S.; Nizami, A.-S.; Khoshnevisan, B.; Mussatto, S.I.; Aghbashlo, M.; Tabatabaei, M.; Lam, S.S. A Comprehensive Review of Engineered Biochar: Production, Characteristics, and Environmental Applications. *J. Clean. Prod.* **2020**, *270*, 122462. [CrossRef]

67. Danish, M.; Ahmad, T. A Review on Utilization of Wood Biomass as a Sustainable Precursor for Activated Carbon Production and Application. *Renew. Sustain. Energy Rev.* **2018**, *87*, 1–21. [CrossRef]
68. Gómez-Serrano, V.; Cuerda-Correa, E.M.; Fernández-González, M.C.; Alexandre-Franco, M.F.; Macías-García, A. Preparation of Activated Carbons from Walnut Wood: A Study of Microporosity and Fractal Dimension. *Smart Mater. Struct.* **2005**, *14*, 363–368. [CrossRef]
69. da Silva Medeiros, D.C.C.; Usman, M.; Chelme-Ayala, P.; Gamal El-Din, M. Biochar-Enhanced Removal of Naphthenic Acids from Oil Sands Process Water: Influence of Feedstock and Chemical Activation. *Energy Environ. Sustain.* **2025**, *1*, 100028. [CrossRef]
70. Ioannidou, O.; Zabaniotou, A. Agricultural Residues as Precursors for Activated Carbon Production—A Review. *Renew. Sustain. Energy Rev.* **2007**, *11*, 1966–2005. [CrossRef]
71. Gale, M.; Nguyen, T.; Moreno, M.; Gilliard-AbdulAziz, K.L. Physiochemical Properties of Biochar and Activated Carbon from Biomass Residue: Influence of Process Conditions to Adsorbent Properties. *ACS Omega* **2021**, *6*, 10224–10233. [CrossRef]
72. Leng, L.; Xiong, Q.; Yang, L.; Li, H.; Zhou, Y.; Zhang, W.; Jiang, S.; Li, H.; Huang, H. An Overview on Engineering the Surface Area and Porosity of Biochar. *Sci. Total Environ.* **2021**, *763*, 144204. [CrossRef] [PubMed]
73. Chun, Y.; Lee, S.K.; Yoo, H.Y.; Kim, S.W. Recent Advancements in Biochar Production According to Feedstock Classification, Pyrolysis Conditions, and Applications: A Review. *BioResources* **2021**, *16*, 6512–6547. [CrossRef]
74. Anderson, N.; Jones, J.; Page-Dumroese, D.; McCollum, D.; Baker, S.; Loeffler, D.; Chung, W. A Comparison of Producer Gas, Biochar, and Activated Carbon from Two Distributed Scale Thermochemical Conversion Systems Used to Process Forest Biomass. *Energies* **2013**, *6*, 164–183. [CrossRef]
75. Kołodyńska, D.; Krukowska, J.; Thomas, P. Comparison of Sorption and Desorption Studies of Heavy Metal Ions from Biochar and Commercial Active Carbon. *Chem. Eng. J.* **2017**, *307*, 353–363. [CrossRef]
76. Chi, N.T.L.; Anto, S.; Ahamed, T.S.; Kumar, S.S.; Shanmugam, S.; Samuel, M.S.; Mathimani, T.; Brindhadevi, K.; Pugazhendhi, A. A Review on Biochar Production Techniques and Biochar Based Catalyst for Biofuel Production from Algae. *Fuel* **2021**, *287*, 119411. [CrossRef]
77. Al-Tohamy, R.; Ali, S.S.; Li, F.; Okasha, K.M.; Mahmoud, Y.A.-G.; Elsamahy, T.; Jiao, H.; Fu, Y.; Sun, J. A Critical Review on the Treatment of Dye-Containing Wastewater: Ecotoxicological and Health Concerns of Textile Dyes and Possible Remediation Approaches for Environmental Safety. *Ecotoxicol. Environ. Saf.* **2022**, *231*, 113160. [CrossRef] [PubMed]
78. Ghodake, G.S.; Shinde, S.K.; Kadam, A.A.; Saratale, R.G.; Saratale, G.D.; Kumar, M.; Palem, R.R.; AL-Shwaiman, H.A.; Elgorban, A.M.; Syed, A.; et al. Review on Biomass Feedstocks, Pyrolysis Mechanism and Physicochemical Properties of Biochar: State-of-the-Art Framework to Speed up Vision of Circular Bioeconomy. *J. Clean. Prod.* **2021**, *297*, 126645. [CrossRef]
79. Alalwan, H.A.; Alminshid, A.H.; Aljaafari, H.A.S. Promising Evolution of Biofuel Generations. Subject Review. *Renew. Energy Focus* **2019**, *28*, 127–139. [CrossRef]
80. Tripathi, M.; Sahu, J.N.; Ganesan, P. Effect of Process Parameters on Production of Biochar from Biomass Waste through Pyrolysis: A Review. *Renew. Sustain. Energy Rev.* **2016**, *55*, 467–481. [CrossRef]
81. Yaashikaa, P.R.; Kumar, P.S.; Varjani, S.; Saravanan, A. A Critical Review on the Biochar Production Techniques, Characterization, Stability and Applications for Circular Bioeconomy. *Biotechnol. Rep.* **2020**, *28*, e00570. [CrossRef] [PubMed]
82. Tomczyk, A.; Sokołowska, Z.; Boguta, P. Biochar Physicochemical Properties: Pyrolysis Temperature and Feedstock Kind Effects. *Rev. Environ. Sci. Bio/Technol.* **2020**, *19*, 191–215. [CrossRef]
83. Fawzy, S.; Osman, A.I.; Yang, H.; Doran, J.; Rooney, D.W. Industrial Biochar Systems for Atmospheric Carbon Removal: A Review. *Environ. Chem. Lett.* **2021**, *19*, 3023–3055. [CrossRef]
84. Kebelmann, K.; Hornung, A.; Karsten, U.; Griffiths, G. Intermediate Pyrolysis and Product Identification by TGA and Py-GC/MS of Green Microalgae and Their Extracted Protein and Lipid Components. *Biomass Bioenergy* **2013**, *49*, 38–48. [CrossRef]
85. Cha, J.S.; Park, S.H.; Jung, S.-C.; Ryu, C.; Jeon, J.-K.; Shin, M.-C.; Park, Y.-K. Production and Utilization of Biochar: A Review. *J. Ind. Eng. Chem.* **2016**, *40*, 1–15. [CrossRef]
86. Singh Siwal, S.; Zhang, Q.; Sun, C.; Thakur, S.; Kumar Gupta, V.; Kumar Thakur, V. Energy Production from Steam Gasification Processes and Parameters That Contemplate in Biomass Gasifier—A Review. *Bioresour. Technol.* **2020**, *297*, 122481. [CrossRef] [PubMed]
87. Chen, D.; Gao, A.; Cen, K.; Zhang, J.; Cao, X.; Ma, Z. Investigation of Biomass Torrefaction Based on Three Major Components: Hemicellulose, Cellulose, and Lignin. *Energy Convers. Manag.* **2018**, *169*, 228–237. [CrossRef]
88. Chen, W.-H.; Biswas, P.P.; Zhang, C.; Kwon, E.E.; Chang, J.-S. Achieving Carbon Credits through Biomass Torrefaction and Hydrothermal Carbonization: A Review. *Renew. Sustain. Energy Rev.* **2025**, *208*, 115056. [CrossRef]
89. Yang, J.; Zhang, Z.; Wang, J.; Zhao, X.; Zhao, Y.; Qian, J.; Wang, T. Pyrolysis and Hydrothermal Carbonization of Biowaste: A Comparative Review on the Conversion Pathways and Potential Applications of Char Product. *Sustain. Chem. Pharm.* **2023**, *33*, 101106. [CrossRef]
90. Kambo, H.S.; Dutta, A. A Comparative Review of Biochar and Hydrochar in Terms of Production, Physico-Chemical Properties and Applications. *Renew. Sustain. Energy Rev.* **2015**, *45*, 359–378. [CrossRef]

91. Razzak, S.A. Municipal Solid and Plastic Waste Derived High-Performance Biochar Production: A Comprehensive Review. *J. Anal. Appl. Pyrolysis* **2024**, *181*, 106622. [CrossRef]
92. Gabhane, J.W.; Bhange, V.P.; Patil, P.D.; Bankar, S.T.; Kumar, S. Recent Trends in Biochar Production Methods and Its Application as a Soil Health Conditioner: A Review. *SN Appl. Sci.* **2020**, *2*, 1307. [CrossRef]
93. Hassan, M.; Liu, Y.; Naidu, R.; Parikh, S.J.; Du, J.; Qi, F.; Willett, I.R. Influences of Feedstock Sources and Pyrolysis Temperature on the Properties of Biochar and Functionality as Adsorbents: A Meta-Analysis. *Sci. Total Environ.* **2020**, *744*, 140714. [CrossRef]
94. Ippolito, J.A.; Cui, L.; Kammann, C.; Wrage-Mönnig, N.; Estavillo, J.M.; Fuertes-Mendizabal, T.; Cayuela, M.L.; Sigua, G.; Novak, J.; Spokas, K.; et al. Feedstock Choice, Pyrolysis Temperature and Type Influence Biochar Characteristics: A Comprehensive Meta-Data Analysis Review. *Biochar* **2020**, *2*, 421–438. [CrossRef]
95. Ge, S.; Yek, P.N.Y.; Cheng, Y.W.; Xia, C.; Wan Mahari, W.A.; Liew, R.K.; Peng, W.; Yuan, T.-Q.; Tabatabaei, M.; Aghbashlo, M.; et al. Progress in Microwave Pyrolysis Conversion of Agricultural Waste to Value-Added Biofuels: A Batch to Continuous Approach. *Renew. Sustain. Energy Rev.* **2021**, *135*, 110148. [CrossRef]
96. Amalina, F.; Razak, A.S.A.; Krishnan, S.; Sulaiman, H.; Zularisam, A.W.; Nasrullah, M. Biochar Production Techniques Utilizing Biomass Waste-Derived Materials and Environmental Applications—A Review. *J. Hazard. Mater. Adv.* **2022**, *7*, 100134. [CrossRef]
97. Adeniyi, A.G.; Iwuozor, K.O.; Emenike, E.C.; Amoloye, M.A.; Adeleke, J.A.; Omonayin, E.O.; Bamigbola, J.O.; Ojo, H.T.; Ezzat, A.O. Leaf-Based Biochar: A Review of Thermochemical Conversion Techniques and Properties. *J. Anal. Appl. Pyrolysis* **2024**, *177*, 106352. [CrossRef]
98. Mohanty, R.; Mahanta, P.; Sharma, R.P. Recent Advances in Biomass Gasification to Improve the Quality of Syngas: A Comprehensive Review. *Ind. Eng. Chem. Res.* **2025**, *64*, 13950–13965. [CrossRef]
99. Cortazar, M.; Santamaria, L.; Lopez, G.; Alvarez, J.; Zhang, L.; Wang, R.; Bi, X.; Olazar, M. A Comprehensive Review of Primary Strategies for Tar Removal in Biomass Gasification. *Energy Convers. Manag.* **2023**, *276*, 116496. [CrossRef]
100. Zahra, A.C.A.; Alahakoon, A.M.Y.W.; Zhu, L.; Prakoso, T.; Abudula, A.; Guan, G. Biochar-Assisted Gasification of Raw Biomass: A Review on the Reactivity and Synergistic Effect on Tar Reforming. *Resour. Chem. Mater.* **2025**, *4*, 100115. [CrossRef]
101. Diyoke, C.; Gao, N.; Aneke, M.; Wang, M.; Wu, C. Modelling of Down-Draft Gasification of Biomass—An Integrated Pyrolysis, Combustion and Reduction Process. *Appl. Therm. Eng.* **2018**, *142*, 444–456. [CrossRef]
102. Lin, S.-L.; Zhang, H.; Chen, W.-H.; Song, M.; Kwon, E.E. Low-Temperature Biochar Production from Torrefaction for Wastewater Treatment: A Review. *Bioresour. Technol.* **2023**, *387*, 129588. [CrossRef]
103. Wang, D.; Jiang, P.; Zhang, H.; Yuan, W. Biochar Production and Applications in Agro and Forestry Systems: A Review. *Sci. Total Environ.* **2020**, *723*, 137775. [CrossRef]
104. Menya, E.; Okello, C.; Storz, H.; Wakatuntu, J.; Turyasingura, M.; Okot, D.K.; Kizito, S.; Komakech, A.J.; Kabenge, I.; Rwahwire, S.; et al. A Review of Progress on Torrefaction, Pyrolysis and Briquetting of Banana Plant Wastes for Biofuels. *Biomass Convers. Biorefinery* **2024**, *15*, 13227–13269. [CrossRef]
105. Yek, P.N.Y.; Cheng, Y.W.; Liew, R.K.; Wan Mahari, W.A.; Ong, H.C.; Chen, W.-H.; Peng, W.; Park, Y.-K.; Sonne, C.; Kong, S.H.; et al. Progress in the Torrefaction Technology for Upgrading Oil Palm Wastes to Energy-Dense Biochar: A Review. *Renew. Sustain. Energy Rev.* **2021**, *151*, 111645. [CrossRef]
106. Wang, Y.; Liu, Y.; Zhang, H.; Duan, X.; Ma, J.; Sun, H.; Tian, W.; Wang, S. Carbonaceous Materials in Structural Dimensions for Advanced Oxidation Processes. *Chem. Soc. Rev.* **2025**, *54*, 2436–2482. [CrossRef]
107. Duan, X.; Sun, H.; Wang, S. Metal-Free Carbocatalysis in Advanced Oxidation Reactions. *Acc. Chem. Res.* **2018**, *51*, 678–687. [CrossRef] [PubMed]
108. Kong, F.; Liu, J.; Xiang, Z.; Fan, W.; Liu, J.; Wang, J.; Wang, Y.; Wang, L.; Xi, B. Degradation of Water Pollutants by Biochar Combined with Advanced Oxidation: A Systematic Review. *Water* **2024**, *16*, 875. [CrossRef]
109. Gupta, A.D.; Singh, H.; Varjani, S.; Awasthi, M.K.; Giri, B.S.; Pandey, A. A Critical Review on Biochar-Based Catalysts for the Abatement of Toxic Pollutants from Water via Advanced Oxidation Processes (AOPs). *Sci. Total Environ.* **2022**, *849*, 157831. [CrossRef]
110. Zeng, Z.; Umeh, A.; Iyengar, G.A.; Qi, F.; Naidu, R. A Critical Review of Different Types of Biochar-Based Catalysts and Mechanisms in Advanced Oxidation Processes for Organic Contaminants Removal. *J. Environ. Chem. Eng.* **2024**, *12*, 114262. [CrossRef]
111. Dai, J.; Wang, Z.; Chen, K.; Ding, D.; Yang, S.; Cai, T. Applying a Novel Advanced Oxidation Process of Biochar Activated Periodate for the Efficient Degradation of Bisphenol A: Two Nonradical Pathways. *Chem. Eng. J.* **2023**, *453*, 139889. [CrossRef]
112. Ruan, X.; Sun, Y.; Du, W.; Tang, Y.; Liu, Q.; Zhang, Z.; Doherty, W.; Frost, R.L.; Qian, G.; Tsang, D.C.W. Formation, Characteristics, and Applications of Environmentally Persistent Free Radicals in Biochars: A Review. *Bioresour. Technol.* **2019**, *281*, 457–468. [CrossRef] [PubMed]
113. Qiao, C.; Jia, W.; Tang, J.; Chen, C.; Wu, Y.; Liang, Y.; Du, J.; Wu, Q.; Feng, X.; Wang, H.; et al. Advances of Carbon-Based Materials for Activating Peracetic Acid in Advanced Oxidation Processes: A Review. *Environ. Res.* **2024**, *263*, 120058. [CrossRef]

114. Yang, H.; Lee, C.-G.; Lee, J. Utilizing Animal Manure-Derived Biochar in Catalytic Advanced Oxidation Processes: A Review. *J. Water Process Eng.* **2023**, *56*, 104545. [CrossRef]
115. Fu, H.; Zhao, P.; Xu, S.; Cheng, G.; Li, Z.; Li, Y.; Li, K.; Ma, S. Fabrication of Fe3O4 and Graphitized Porous Biochar Composites for Activating Peroxymonosulfate to Degrade P-Hydroxybenzoic Acid: Insights on the Mechanism. *Chem. Eng. J.* **2019**, *375*, 121980. [CrossRef]
116. Zhao, B.; O'Connor, D.; Zhang, J.; Peng, T.; Shen, Z.; Tsang, D.C.W.; Hou, D. Effect of Pyrolysis Temperature, Heating Rate, and Residence Time on Rapeseed Stem Derived Biochar. *J. Clean. Prod.* **2018**, *174*, 977–987. [CrossRef]
117. Pan, X.; Gu, Z.; Chen, W.; Li, Q. Preparation of Biochar and Biochar Composites and Their Application in a Fenton-like Process for Wastewater Decontamination: A Review. *Sci. Total Environ.* **2021**, *754*, 142104. [CrossRef]
118. Smith, M.B.; March, J. *March's Advanced Organic Chemistry: Reactions, Mechanisms, and Structure*, 6th ed.; John Wiley & Sons: Hoboken, NJ, USA, 2007; pp. 1737–1742. ISBN 9780470084946.
119. Harries, C. Über Die Einwirkung Des Ozons Auf Organische Verbindungen. In *Untersuchungen Über das Ozon und Seine Einwirkung auf Organische Verbindungen (1903–1916)*; Springer: Berlin/Heidelberg, Germany, 1916; pp. 266–286.
120. Criegee, R. Mechanism of Ozonolysis. *Angew. Chem. Int. Ed. Engl.* **1975**, *14*, 745–752. [CrossRef]
121. Rieche, A.; Meister, R.; Sauthoff, H. Über Ozonide Und Ihre Spaltung. *Justus Liebigs Ann. Chem.* **1942**, *553*, 187–249. [CrossRef]
122. Criegee, R.; Wenner, G. Die Ozonisierung Des 9,10-Oktalins. *Justus Liebigs Ann. Chem.* **1949**, *564*, 9–15. [CrossRef]
123. Criegee, R. Über Den Verlauf Der Ozonspaltung (III. Mitteilung). *Justus Liebigs Ann. Chem.* **1953**, *583*, 1–36. [CrossRef]
124. Hassan, Z.; Stahlberger, M.; Rosenbaum, N.; Bräse, S. Criegee Intermediates Beyond Ozonolysis: Synthetic and Mechanistic Insights. *Angew. Chem. Int. Ed.* **2021**, *60*, 15138–15152. [CrossRef] [PubMed]
125. Chiavola, A.; Marcantonio, C.D.; Noè Porretti, A.; Scagnetti, S.; Ciuchi, V.; Boni, M.R.; Micoli, S.; Lazzazzara, M.; Leoni, S.; Frugis, A.; et al. Application of Adsorption and Ozonation as Quaternary Treatment of WWTP Effluent for the Removal of Contaminants of Emerging Concern: Results from Laboratory Scale Experiments. *J. Hazard. Mater. Adv.* **2025**, *18*, 100665. [CrossRef]
126. Akmehmet Balcıoğlu, I.; Ötker, M. Treatment of Pharmaceutical Wastewater Containing Antibiotics by O_3 and O_3/H_2O_2 Processes. *Chemosphere* **2003**, *50*, 85–95. [CrossRef]
127. Ratnawati, R.; Enjarlis, E.; Husnil, Y.A.; Christwardana, M.; Slamet, S. Degradation of Phenol in Pharmaceutical Wastewater Using TiO2/Pumice and O3/Active Carbon. *Bull. Chem. React. Eng. Catal.* **2019**, *15*, 146–154. [CrossRef]
128. Patel, S.; Agarwal, R.; Majumder, S.K.; Das, P.; Ghosh, P. Kinetics of Ozonation and Mass Transfer of Pharmaceuticals Degraded by Ozone Fine Bubbles in a Plant Prototype. *Heat Mass Transf.* **2019**, *56*, 385–397. [CrossRef]
129. Selvam, K.; Swaminathan, K.; Chae, K. Microbial Decolorization of Azo Dyes and Dye Industry Effluent by Fomes Lividus. *World J. Microbiol. Biotechnol.* **2003**, *19*, 591–593. [CrossRef]
130. Mao, Y.; Guan, Y.; Luo, D.; Zheng, Q.; Feng, X.; Wang, X. Investigation of a Homogeneous Activating Ozonation Method in the Rinsing Procedure of Cotton Fabric Dyed with Reactive Dye. *Color. Technol.* **2011**, *127*, 256–267. [CrossRef]
131. Bilińska, L.; Blus, K.; Foszpańczyk, M.; Gmurek, M.; Ledakowicz, S. Catalytic Ozonation of Textile Wastewater as a Polishing Step after Industrial Scale Electrocoagulation. *J. Environ. Manag.* **2020**, *265*, 110502. [CrossRef]
132. Sunitha, S.; Rao, A.N. ZnO/Carbon Nano Composite: Effective Catalyst for the Photo Degradation of Acid Blue 113. In Proceedings of the CARBON MATERIALS 2012 (CCM12): Carbon Materials for Energy Harvesting, Environment, Nanoscience and Technology, Mumbai, India, 1–3 November 2012; pp. 151–156.
133. Kaur, S.; Singh, V. TiO2 Mediated Photocatalytic Degradation Studies of Reactive Red 198 by UV Irradiation. *J. Hazard. Mater.* **2007**, *141*, 230–236. [CrossRef]
134. Rahimi, S.; Ehrampoush, M.H.; Ghaneian, M.T.; Reshadat, S.; Fatehizadeh, A.; Ahmadian, M.; Ghanizadeh, G.; Rahimi, S. Application of TiO_2/UV-C Photocatalytic Process in Removal of Reactive Red 198 Dye from Synthetic Textile Wastewater. *Asian J. Chem.* **2013**, *25*, 7427–7432. [CrossRef]
135. Joshi, A.U.; Hinsu, A.T.; Kotadiya, R.J.; Rank, J.K.; Andharia, K.N.; Kothari, R.K. Decolorization and Biodegradation of Textile Di-Azo Dye Acid Blue 113 by *Pseudomonas stutzeri* AK6. *3 Biotech* **2020**, *10*, 214. [CrossRef] [PubMed]
136. Kumar Singh, P.; Pratap Singh, R.; Singh, P.; Lakhan Singh, R. Efficient Decolorization of Dye Acid Blue 113 by Soil Bacterium *Bacillus subtilis* RMLP2. *Toxicol. Int.* **2021**, *28*, 267–278. [CrossRef]
137. Karimi, A.; Mahdizadeh, F.; Eskandarian, M. Enzymatic In-Situ Generation of H_2O_2 for Decolorization of Acid Blue 113 by Fenton Process. *Chem. Ind. Chem. Eng. Q.* **2012**, *18*, 89–94. [CrossRef]
138. Soares, O.S.G.P.; Faria, P.C.C.; Órfão, J.J.M.; Pereira, M.F.R. Ozonation of Textile Effluents and Dye Solutions in the Presence of Activated Carbon under Continuous Operation. *Sep. Sci. Technol.* **2007**, *42*, 1477–1492. [CrossRef]
139. Adams, C.D.; Gorg, S. Effect of pH and Gas-Phase Ozone Concentration on the Decolorization of Common Textile Dyes. *J. Environ. Eng.* **2002**, *128*, 293–298. [CrossRef]
140. Zheng, Q.; Dai, Y.; Han, X. Decolorization of Azo Dye C.I. Reactive Black 5 by Ozonation in Aqueous Solution: Influencing Factors, Degradation Products, Reaction Pathway and Toxicity Assessment. *Water Sci. Technol.* **2015**, *73*, 1500–1510. [CrossRef]

141. Wantoputri, N.; Notodarmojo, S.; Helmy, Q. Reactive Black-5 Removal by Ozonation as Post Treatment. In *IOP Conference Series: Materials Science and Engineering, Proceedings of the International Conference on Science and Innovated Enginnering (I-COSINE), Aceh, Indonesia, 21–22 October 2018*; IOP: Bristol, UK, 2018. [CrossRef]
142. Faria, P.C.C.; Órfão, J.J.M.; Pereira, M.F.R. Ozone Decomposition in Water Catalyzed by Activated Carbon: Influence of Chemical and Textural Properties. *Ind. Eng. Chem. Res.* **2006**, *45*, 2715–2721. [CrossRef]
143. He, Z.; Song, S.; Zhou, H.; Ying, H.; Chen, J.C.I. Reactive Black 5 Decolorization by Combined Sonolysis and Ozonation. *Ultrason. Sonochem.* **2007**, *14*, 298–304. [CrossRef]
144. Kumar, M.P.G.; Ishii, S.; Müller, T.S.; Itoh, K.; Murabayashi, M. Treatment of Textile Dye Wastewater Using Ozone Combined with Photocatalyst. *Toxicol. Environ. Chem.* **1999**, *68*, 221–231. [CrossRef]
145. El-Dein, A.M.; Libra, J.; Wiesmann, U. Cost Analysis for the Degradation of Highly Concentrated Textile Dye Wastewater with Chemical Oxidation H_2O_2/UV and Biological Treatment. *J. Chem. Technol. Biotechnol.* **2006**, *81*, 1239–1245. [CrossRef]
146. Pirgalıoğlu, S.; Özbelge, T.A. Comparison of Non-Catalytic and Catalytic Ozonation Processes of Three Different Aqueous Single Dye Solutions with Respect to Powder Copper Sulfide Catalyst. *Appl. Catal. A Gen.* **2009**, *363*, 157–163. [CrossRef]
147. Chen, H.-W.; Kuo, Y.-L.; Chiou, C.-S.; You, S.-W.; Ma, C.-M.; Chang, C.-T. Mineralization of Reactive Black 5 in Aqueous Solution by Ozone/H_2O_2 in the Presence of a Magnetic Catalyst. *J. Hazard. Mater.* **2010**, *174*, 795–800. [CrossRef]
148. Wu, D.; Liu, Y.; He, H.; Zhang, Y. Magnetic Pyrite Cinder as an Efficient Heterogeneous Ozonation Catalyst and Synergetic Effect of Deposited Ce. *Chemosphere* **2016**, *155*, 127–134. [CrossRef]
149. Pérez, A.; Rodríguez, J.L.; Galicia, A.; Chairez, I.; Poznyak, T. Recycling Strategy for Water Contaminated with Reactive Black 5 in the Presence of Additives Treated by Simple Ozonation. *Ozone Sci. Eng.* **2018**, *41*, 46–59. [CrossRef]
150. Pérez, A.; Poznyak, T.; Chairez, I. Effect of Additives on Ozone-Based Decomposition of Reactive Black 5 and Direct Red 28 Dyes. *Water Environ. Res.* **2013**, *85*, 291–300. [CrossRef]
151. Wang, X.; Cheng, X.; Sun, D.; Ren, Y.; Xu, G. Fate and Transformation of Naphthylaminesulfonic Azo Dye Reactive Black 5 during Wastewater Treatment Process. *Environ. Sci. Pollut. Res.* **2014**, *21*, 5713–5723. [CrossRef] [PubMed]
152. Ebrahimpour, Z.; Pliekhova, O.; Cabrera, H.; Abdelhamid, M.; Korte, D.; Segbéya Gadedjisso-Tossou, K.; Niemela, J.; Lavrencic Stangar, U.; Franko, M. Photodegradation Mechanisms of Reactive Blue 19 Dye under UV and Simulated Solar Light Irradiation. *Spectrochim. Acta Part A Mol. Biomol. Spectrosc.* **2021**, *252*, 119481. [CrossRef]
153. Holkar, C.R.; Pandit, A.B.; Pinjari, D.V. Kinetics of Biological Decolorisation of Anthraquinone Based Reactive Blue 19 Using an Isolated Strain of Enterobacter Sp.F NCIM 5545. *Bioresour. Technol.* **2014**, *173*, 342–351. [CrossRef] [PubMed]
154. Lovato, M.E.; Fiasconaro, M.L.; Martín, C.A. Degradation and Toxicity Depletion of RB19 Anthraquinone Dye in Water by Ozone-Based Technologies. *Water Sci. Technol.* **2016**, *75*, 813–822. [CrossRef]
155. Tehrani-Bagha, A.R.; Mahmoodi, N.M.; Menger, F.M. Degradation of a Persistent Organic Dye from Colored Textile Wastewater by Ozonation. *Desalination* **2010**, *260*, 34–38. [CrossRef]
156. Lall, R.; Mutharasan, R.; Shah, Y.T.; Dhurjati, P. Decolorization of the Dye, Reactive Blue 19, Using Ozonation, Ultrasound, and Ultrasound-Enhanced Ozonation. *Water Environ. Res.* **2003**, *75*, 171–179. [CrossRef] [PubMed]
157. Malakootian, M.; Honarmandrad, Z. Investigating the Use of Ozonation Process with Calcium Peroxide for the Removal of Reactive Blue 19 Dye from Textile Wastewater. *Desalination Water Treat.* **2018**, *118*, 336–341. [CrossRef]
158. Kaur, N.; Kaur, S.; Singh, V. Preparation, Characterization and Photocatalytic Degradation Kinetics of Reactive Red Dye 198 Using N, Fe Codoped TiO_2 Nanoparticles under Visible Light. *Desalination Water Treat.* **2016**, *57*, 9237–9246. [CrossRef]
159. Ghadim, E.E.; Lamei, N.; Panahyab, A.; Hatefi, M.; Abdi, K. Decolorization and Removal of Reactive Red 198 by Nano-Magnetic Graphene Oxide. *Asian J. Chem.* **2017**, *29*, 715–722. [CrossRef]
160. Akar, S.T.; Akar, T.; Çabuk, A. Decolorization of a Textile Dye, Reactive Red 198 (Rr198), by Aspergillus Parasiticus Fungal Biosorbent. *Braz. J. Chem. Eng.* **2009**, *26*, 399–405. [CrossRef]
161. Thangaraj, S.; Bankole, P.O.; Sadasivam, S.K.; Kumarvel, V. Biodegradation of Reactive Red 198 by Textile Effluent Adapted Microbial Strains. *Arch. Microbiol.* **2021**, *204*, 12. [CrossRef] [PubMed]
162. Mahdizadeh, H.; Dadban Shahamat, Y.; Rodríguez-Couto, S. Discoloration and Mineralization of a Textile Azo Dye Using a Hybrid UV/O3/SBR Process. *Appl. Water Sci.* **2021**, *11*, 159. [CrossRef]
163. Ghaneian, M.T. Application of Ozonation Process for the Removal of Reactive Red 198 Dye from Aqueous Solutions. *Iran. J. Energy Environ.* **2011**, *13*, 1909–1915. [CrossRef]
164. Mohan, S.; Oke, N. Application of the Optimized Pre-Ozonation Treatment for Potential Resource Recovery from Industrial Textile Effluent. *Ozone Sci. Eng.* **2021**, *44*, 236–249. [CrossRef]
165. Ehrampoush, M.H.; Miri, M.; Momtaz, S.M.; Ghaneian, M.T.; Rafati, L.; Karimi, H.; Rahimi, S. Selecting the Optimal Process for the Removal of Reactive Red 198 Dye from Textile Wastewater Using Analytical Hierarchy Process (AHP). *Desalination Water Treat.* **2016**, *57*, 27237–27242. [CrossRef]
166. Babel, S. Low-Cost Adsorbents for Heavy Metals Uptake from Contaminated Water: A Review. *J. Hazard. Mater.* **2003**, *97*, 219–243. [CrossRef]

167. 164; Zhao, R. A Review on the Catalytic Ozonation of Pollutants in Wastewater by Heteroelements-Doped Biochar: Internal and External Doping Strategies. *Alex. Eng. J.* **2025**, *119*, 35–44. [CrossRef]
168. Wang, J.; Duan, X.; Nanayakkara, N.; Liu, Y. Transforming Organics via Polymerization Pathway in Advanced Oxidation Processes: A Review. *Energy Environ. Sustain.* **2025**, *1*, 100006. [CrossRef]
169. Li, Y.; Li, Y.; Ni, B.-J.; Li, Y.-Z.; Ni, S.-Q. Towards Scalable Anammox: Mechanistic Insights and Emerging Strategies. *Trends Biotechnol.* **2025**. [CrossRef] [PubMed]
170. Zhu, X.; Yang, F.; Pang, Q.; Peng, F.; Xu, B.; Wang, L.; Xie, L.; Zhang, W.; Tian, L.; Hou, J.; et al. Fluvial Dissolved Organic Matter Quality Modulates Microbial Nitrate Transformation: Enhanced Denitrification under Low Carbon-to-Nitrate Ratio. *Environ. Sci. Technol.* **2025**, *59*, 23456–23465. [CrossRef]